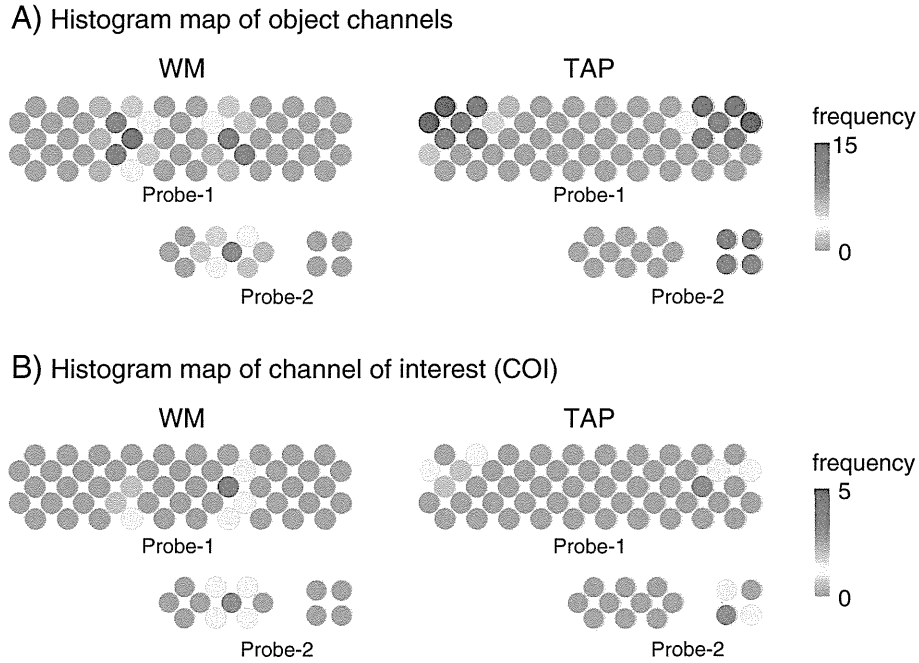

Fig. 4. Histogram maps of (A) object channels and (B) channel of interest. In (A), number of participants whose registration was in a target BA (BA 46 for WM task; BAs 1, 2, 3, 4, 5, 6, and 40 for TAP task) is indicated by frequency represented by color scale for each NIRS channel. In (B), number of participants in selected channel is indicated by color scale for each channel. Arrangement of NIRS channels on head is shown in Fig. 1.

discovery rate (FDR) control procedure (Genovese et al., 2002) (FDR corrected $p < 0.05$). The total numbers of voxels and correlated voxels were determined for both the GM and ST regions. A two-way analysis of variance (ANOVA) (layer × task) was used to examine the difference by layer type (GM or ST) and by task type (WM or TAP) for oxy- and deoxy-Hb signals.

(2) Correlation with L-BOLD signals
The continuous L-BOLD signals in the GM and ST layers (L-BOLD (GM) and L-BOLD (ST) signals) were used to calculate the correlation coefficients for the NIRS-Hb signals for each task (Step B-9). In addition, an LDF signal was used to calculate the correlation coefficients for the NIRS-Hb signals. For statistical examination, correlation coefficient r was converted into a Z-value using Fisher's Z-transformation (Eq. (4))(Fisher, 1915, 1921):

$$Z = \frac{1}{2}\ln\frac{1+r}{1-r}. \quad (4)$$

The correlation Z-values were tested using a one-sample t test against zero. The significance of the t-values under all conditions was determined by using a threshold corrected for multiple comparisons using the Bonferroni procedure (Bonferroni corrected $p < 0.05$, two-tailed).

(3) Correlation analysis for block-averaged activation signals
To examine the correlation of the task-related responses in more detail, we calculated time-locked block-averaged timecourses for the NIRS, L-BOLD, and LDF signals for each task condition and each participant (Step B-10). First, the time-continuous data were separated into task blocks: a WM task block was defined as 14 scans (35-s) period starting 2 scans (5-s) before the Target onset and ending 12 scans (30-s) after the onset, and a TAP task block was defined as 17 scans (42.5-s) period starting 3 scans (7.5-s) before the task onset and ending 14 scans (35-s) after the onset. Each task block was shifted to make the average value during the pre-task period (including the task onset) zero as the baseline. Then, the task blocks were averaged for each task and each participant and used as the block-averaged signals. Using the block-averaged signals, we calculated the task-related response amplitudes as the average value during the activation periods. The activation period for the WM task was defined as three scans (7.5 s) from the second scan after Target onset, and that for the TAP task was defined as five scans (12.5 s) from the third scan after task onset. To examine the linearity of the response amplitudes between the NIRS and L-BOLD signals, we calculated the correlation coefficients across participants. We additionally calculated effect sizes using Eq. (2) and data from before the averaging process to examine the signal-to-noise ratio (SNR) for the task-related response for each signal.

Correlation analysis for multiple NIRS channels

The correlation coefficients between the continuous NIRS and L-BOLD (GM) signals were calculated for all NIRS channels in the Probe-1 data to examine the generality and spatial variability of the correlation between the NIRS and fMRI signals (Step B-11). On the basis of the correlation coefficients under four conditions (oxy-Hb in WM, deoxy-Hb in WM, oxy-Hb in TAP, deoxy-Hb in TAP), the 52 NIRS channels were clustered into three areas using K-means clustering in MATLAB (MathWorks, Inc., U.S.A.) to determine the area dependency of the correlation coefficients.

Results

Selection of COI

The BA number was determined for each NIRS channel for each participant in accordance with the registration of NIRS channels in the MNI space (Table 1). Frequency maps of the object NIRS channels (BA 46 for WM task; BAs 1, 2, 3, 4, 5, 6, and 40 for TAP task) showed that both probe holders covered the regions of interest, i.e., the dorsolateral PFC and the sensorimotor cortex (Fig. 4A). A COI was not

Table 1
Estimated location of each NIRS channel in Probe-1 and Probe-2 on normalized brain image. Mean and standard deviation (SD) of MNI coordinates across participants and corresponding Brodmann area (BA) numbers are shown for each channel. Percentage of participants by BA number is shown in parentheses.

Ch	Mean MNI coordinates			SD		BA (%)	
	x	y	z				
Probe-1							
1	58.8	−22.5	51.3	5.1	3 (40%)	1 (40%)	2, 4, 6 (7%)
2	54.3	0.4	49.5	6.5	6 (80%)	4 (13%)	44 (7%)
3	44.8	23.2	47.9	6.2	9 (73%)	45 (13%)	6, 46 (7%)
4	30.0	40.0	46.7	6.3	9 (67%)	8 (20%)	46 (13%)
5	10.3	50.1	46.8	7.3	9 (80%)	8 (13%)	10 (7%)
6	−8.9	50.0	46.7	6.9	9 (87%)	8 (7%)	10 (7%)
7	−29.1	38.3	46.4	5.2	9 (80%)	46 (13%)	8 (7%)
8	−44.1	20.9	47.5	5.7	9 (87%)	45 (13%)	-
9	−53.3	−0.4	48.0	7.0	6 (93%)	44 (7%)	-
10	−58.5	−25.5	48.9	5.4	3 (40%)	2, 40 (20%)	1 (13%)
11	64.1	−34.3	43.5	3.9	40 (73%)	2 (20%)	1 (7%)
12	62.8	−7.7	39.2	5.3	3 (40%)	1 (27%)	6 (20%)
13	55.5	17.1	36.8	4.8	44 (47%)	6 (33%)	45 (13%)
14	43.7	38.7	35.1	5.7	46 (67%)	45 (20%)	9 (13%)
15	23.1	54.9	35.3	6.3	9 (73%)	46 (20%)	10 (7%)
16	1.6	59.2	36.4	4.6	9 (73%)	10 (27%)	-
17	−22.5	53.9	35.3	5.9	9 (67%)	46 (27%)	10 (7%)
18	−42.4	37.5	34.1	5.5	45 (47%)	46 (40%)	9 (13%)
19	−53.7	15.2	36.3	5.5	44 (53%)	9 (27%)	45 (13%)
20	−62.0	−10.5	37.6	5.2	1 (47%)	43 (27%)	3 (13%)
21	−62.9	−36.0	41.9	4.0	40 (87%)	2 (13%)	-
22	67.7	−19.3	30.5	3.3	2 (73%)	43 (13%)	1 (13%)
23	63.1	7.9	26.5	4.1	6 (73%)	4, 43, 44, 45 (7%)	
24	53.3	33.3	24.0	5.9	45 (80%)	44 (13%)	46 (7%)
25	36.8	54.3	23.9	4.6	46 (93%)	10 (7%)	-
26	12.5	65.3	24.0	5.1	10 (93%)	9 (7%)	-
27	−12.1	64.4	24.7	5.3	10 (87%)	9 (13%)	-
28	−36.4	52.5	23.1	5.6	46 (87%)	10 (13%)	-
29	−51.6	32.4	22.5	5.4	45 (100%)	-	-
30	−61.2	6.4	24.7	5.5	6 (73%)	43 (20%)	44 (7%)
31	−66.0	−21.2	29.2	4.7	2 (67%)	43 (27%)	40 (7%)
32	69.6	−32.0	13.6	3.4	22 (87%)	2, 40 (7%)	-
33	67.2	−4.3	13.6	3.5	22 (40%)	43 (33%)	48 (27%)
34	58.8	26.3	11.9	3.6	45 (67%)	44 (33%)	-
35	46.9	49.7	10.1	4.8	46 (80%)	45 (13%)	10 (7%)
36	25.6	65.5	11.2	4.9	10 (67%)	11 (20%)	46 (13%)
37	−0.5	68.8	11.6	4.3	10 (93%)	11 (7%)	-
38	−25.7	64.1	11.6	4.9	10 (87%)	11, 46 (7%)	-
39	−45.7	48.4	9.2	4.5	46 (80%)	45 (20%)	-
40	−57.2	25.1	10.8	5.8	45 (67%)	44 (27%)	47 (7%)
41	−65.1	−6.5	11.9	4.5	43 (40%)	22 (33%)	21 (7%)
42	−67.6	−34.7	13.3	5.0	22 (80%)	21 (13%)	48 (7%)
43	69.7	−16.9	−4.0	2.2	21 (60%)	22 (40%)	-
44	60.7	10.5	−3.1	4.6	38 (40%)	48 (40%)	21 (20%)
45	52.9	41.2	−3.5	3.8	46 (47%)	45 (40%)	47 (13%)
46	38.3	60.3	−1.3	3.4	10 (60%)	46, 47 (20%)	-
47	14.9	69.3	−0.7	3.7	11 (53%)	10 (47%)	-
48	−13.7	69.1	0.0	4.3	10 (53%)	11 (47%)	-
49	−37.7	59.3	−1.7	3.8	10 (73%)	47 (20%)	46 (7%)
50	−52.0	38.9	−3.9	3.6	45 (73%)	47 (27%)	-
51	−59.6	8.0	−3.5	5.3	48 (40%)	38 (33%)	21 (20%)
52	−67.7	−18.8	−5.1	4.5	21 (67%)	22 (33%)	-
Probe-2							
1	−5.8	57.8	38.5	4.2	9 (83%)	10 (17%)	-
2	−24.7	50.7	37.7	4.7	9 (58%)	46 (42%)	-
3	−42.5	36.8	34.7	4.2	45 (42%)	46 (33%)	9 (25%)
4	5.5	65.2	25.7	4.8	10 (92%)	9 (8%)	-
5	−15.0	62.2	27.2	4.9	10 (67%)	9 (17%)	46 (17%)
6	−36.2	50.7	26.2	4.5	46 (83%)	45 (17%)	-
7	−50.7	34.3	21.8	4.4	45 (83%)	46 (8%)	44 (8%)
8	−7.2	68.7	14.5	4.8	10 (100%)	-	-
9	−27.3	62.5	15.0	4.0	10 (75%)	46 (25%)	-
10	−44.5	48.8	12.2	3.9	46 (50%)	45 (42%)	10 (8%)
11	−52.0	−23.3	57.0	5.5	3 (33%)	4 (33%)	1, 40 (17%)
12	−48.0	−37.8	59.2	3.9	40 (58%)	3 (33%)	1 (8%)
13	−61.5	−29.0	44.7	4.7	40 (42%)	2, 3 (25%)	1 (8%)
14	−56.5	−46.5	48.0	4.0	40 (83%)	39 (17%)	-

selected for 8 participants in the WM task and 11 participants in the TAP task because there were no channels meeting the two criteria described above. Failure to meet the first criteria resulted from a failure to detect enough light power in the TAP task (eight participants showed no object channels with sufficient light power), possibly because the sensorimotor area corresponded to haired regions. Failure to meet the threshold of effect size resulted from a failure to detect a reliable response to the task. This resulted in the removal of eight participants from the WM task data and three participants from the TAP task data. We thus analyzed the COI signals for 19 and 16 participants for the WM and TAP tasks, respectively (Fig. 4B). The results of correlation analysis using the COI data are presented in the following sub-sections.

Correlation of NIRS-Hb signals with BOLD and LDF signals for COI

Temporal correlation of NIRS-Hb signals with voxel-level BOLD signals

First, to investigate the general tendency, we compared the continuous data, i.e., the data for the entire duration of the experiment, between the NIRS and BOLD signals. Representative results for two participants are shown in Fig. 5. Voxel-level correlation analysis revealed that the majority of GM voxels in the SFA had significant correlation coefficients for both the WM (Fig. 5A) and TAP (Fig. 5C) tasks whereas only a few ST voxels had significant coefficients. Moreover, the L-BOLD (GM) signals were highly correlated with both the oxy-Hb and deoxy-Hb signals within participant (Figs. 5B and D).

The mean data values for the voxel-level analysis for the participants with a COI are shown in Table 2. A two-way ANOVA (layer type×task type) for the total number of voxels showed a significant interaction between layer type and task type (F (1, 66) = 11.4, $p < 0.005$) without any main effects (layer type: F (1, 66) = 3.4, $p = 0.07$; task type: F (1, 66) = 2.3, $p = 0.13$). This means that the total number of voxels was larger for ST than for GM in the sensorimotor area (TAP task) and that the opposite case held for the PFC (WM task). Nonetheless, the number of correlated voxels for GM (mean = 118–162) was clearly larger than that for ST (mean 7–17) for both tasks (Table 2). The two-way ANOVA (layer type×task type) for the number of correlated voxels revealed a clear significance for the main effects of layer signal (F (1, 66) = 59.1 for oxy-Hb and F (1, 66) = 37.0 for deoxy-Hb, $p < 0.00001$) without the main effects of task type (F (1, 66) = 1.5, $p = 0.22$ for oxy-Hb and F (1, 66) = 0.2, $p = 0.67$ for deoxy-Hb) or interaction (F (1, 66) = 2.3, $p = 0.14$ for oxy-Hb and F (1, 66) = 0.0, $p = 0.94$ for deoxy-Hb).

Temporal correlation of NIRS-Hb signals with L-BOLD and LDF signals in continuous data

The correlation coefficients of the NIRS-Hb signals for the L-BOLD (GM), L-BOLD (ST), and LDF signals were statistically examined across participants (Fig. 6). First, the Z-values for each condition were tested by performing a one-sample t-test against zero across participants in which the p-value was corrected for the multiple (12×) comparisons. On the one hand, the L-BOLD (GM) signals showed significant correlation coefficients with the oxy-Hb signals (WM: $t(18) = 8.2$, $p < 5 \times 10^{-6}$; TAP: $t(15) = 4.8$, $p < 5 \times 10^{-3}$) and with the deoxy-Hb signals (WM: $t(18) = 4.4$, $p < 5 \times 10^{-3}$; TAP: $t(15) = 5.2$, $p < 5 \times 10^{-3}$) (Fig. 6A). The two-way ANOVA (task type × Hb type) showed a generality of the NIRS–BOLD relationship as no main effect of task type ($p = 0.37$) and Hb type ($p = 0.24$) with no interaction ($p = 0.73$) were indicated. On the other hand, the L-BOLD (ST) signals showed no significant correlation coefficients with any of the NIRS-Hb signals ($p > 0.2$) (Fig. 6B).

Because use of the extracranial BOLD signal has not become standard, the same correlation analysis was conducted using LDF signals instead of L-BOLD signals (Fig. 6C). As the temporal LDF signals in the two channels were significantly correlated within participants in most cases (mean ± SD of $r = 0.52 \pm 0.22$, $p < 0.0001$ for 25 of 27 participants), only the LDF signal in channel 1 (centered between

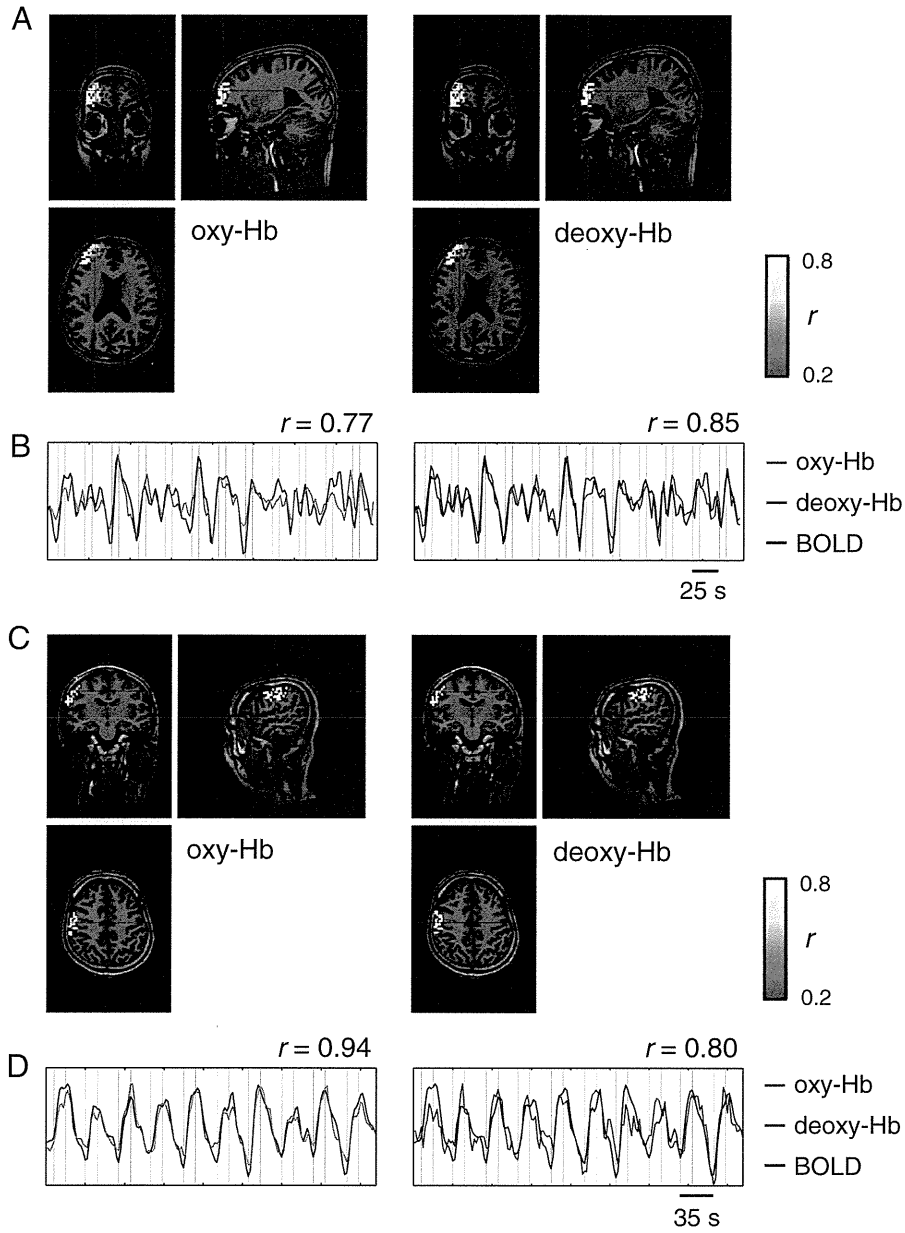

Fig. 5. Examples of correlation between NIRS-Hb signals and BOLD signals. (A) Example for WM task. Significantly correlated voxels ($p < 0.05$, FDR corrected for total number of object voxels) were superimposed on T1-weighted image. Sign of correlation coefficients for NIRS deoxy-Hb signals was inverted for comparison with result for NIRS oxy-Hb signals. (B) Time courses of NIRS oxy-Hb (red line) and NIRS deoxy-Hb signals (blue line) along with that for L-BOLD signal in GM (black), which corresponds to example (A). Sign of NIRS deoxy-Hb signal was inverted for comparison with L-BOLD signal. NIRS-Hb and L-BOLD signals were normalized to have the same range of amplitude and are shown in arbitrary units. (C) and (D) Example for TAP task, which is shown in the same manner as in (A) and (B).

the eyebrows) was used here. The results for LDF channel 2 were basically the same, as shown in the Supplementary Materials (Fig. S1). A one-sample *t*-test against zero indicated significant correlation coefficients only for the oxy-Hb signals for the WM task ($t(18) = 5.4$, $p < 5 \times 10^{-3}$). To investigate the dominance of the L-BOLD (GM) signals compared to the LDF signals for contribution to the oxy-Hb signals, we conducted a two-way ANOVA between signal type (L-BOLD (GM)/LDF) and task type (WM/TAP) for the correlation *Z*-values. The results revealed a significant main effect of signal type (F (1, 66) = 13.6, $p < 5 \times 10^{-4}$) with no main effect of task ($p = 0.91$) and no interaction ($p = 0.45$), indicating that the correlation between the NIRS oxy-Hb and L-BOLD (GM) signals was higher than that between the NIRS oxy-Hb and LDF signals.

Table 2
Basic results of voxel-based BOLD analysis for channel of interest.

	Gray matter		Soft tissue	
	WM	TAP	WM	TAP
Number of total voxels	266 ± 65	229 ± 89	235 ± 80	336 ± 107
Number of voxels correlated with oxy-Hb signals ± SD (Percentage ± SD)	162 ± 102 (58 ± 32%)	118 ± 86 (58 ± 41%)	12 ± 14 (6 ± 8%)	17 ± 18 (6 ± 8%)
Number of voxels correlated with deoxy-Hb signals ± SD (Percentage ± SD)	119 ± 117 (45 ± 42%)	128 ± 97 (66 ± 35%)	7 ± 9 (4 ± 6%)	13 ± 20 (6 ± 10%)

Correlation of NIRS-Hb signals with L-BOLD and LDF signals in block-averaged data

To further examine the relationship between the NIRS-Hb and L-BOLD (GM) signals, we calculated the time-locked block-averaged

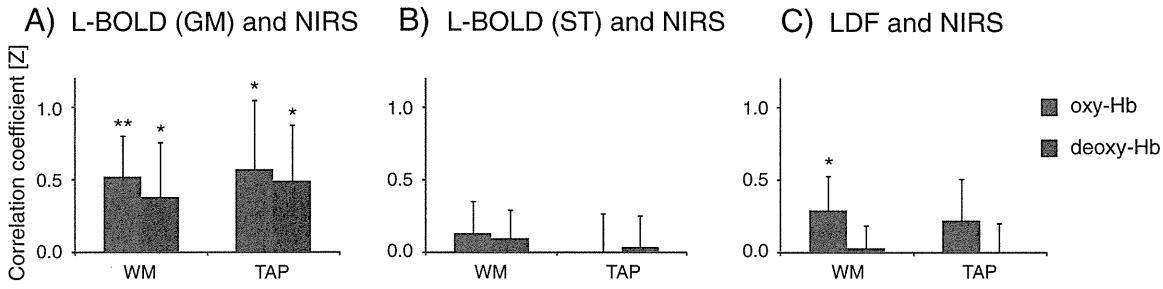

Fig. 6. Mean and standard deviation of correlation coefficients (*Z*-values from Fisher's transformation) for NIRS-Hb signals in activation area for WM task (n = 19) and TAP task (n = 16). (A) Correlation of L-BOLD signals in GM region with NIRS-Hb signals. (B) Correlation of L-BOLD signals in ST region with NIRS-Hb signals. (C) Correlation of LDF signals with NIRS-Hb signals. Sign of correlation coefficients for NIRS deoxy-Hb signals was inverted for comparison with results for oxy-Hb signals. Statistical significance against zero is shown ($^{**}p < 5 \times 10^{-6}$, $^{*}p < 5 \times 10^{-3}$). Bonferroni correction was applied for multiple comparisons.

timecourses as they represent purer task-related responses for each participant. The mean and standard error of the block-averaged timecourses across participants are shown not only for the NIRS-Hb and L-BOLD (GM) signals but also for L-BOLD (ST) and LDF signals (Fig. 7). In addition, the task-related signal changes were quantified by the effect size (Table 3). For both tasks, the NIRS oxy-Hb signals clearly increased along with an increase in the L-BOLD (GM) signals and a decrease in the NIRS deoxy-Hb signals. On the other hand, the L-BOLD (ST) signals tended to increase for the WM task and to decrease for the TAP task. In addition, the LDF signals for the WM task showed a clear increase for the WM task. The correlation coefficients for the block-averaged timecourses in different modalities, which are listed in Table 4, showed a tendency similar to the results shown by the continuous data (Fig. 6) as expected. In short, the L-BOLD (GM) signals showed a high correlation with the NIRS-Hb signals (mean $|r| > 0.5$) while the L-BOLD (ST) signals did not show such a tendency (mean $|r| < 0.22$). In addition, the LDF signals showed a high correlation with only the NIRS oxy-Hb signal for the WM task (mean $r = 0.52 \pm 0.46$) (Table 4).

Using the block-averaged timecourses, we compared the amplitudes of the task-related responses between the NIRS-Hb and L-BOLD (GM) signals (Fig. 8). For both tasks, the two signals showed significant correlation ($p < 0.05$), which means the participants with a stronger response in the NIRS-Hb signal also showed a stronger response in the L-BOLD (GM) signal in the fMRI data. Note that these block-averaged results were not due to a biased selection of participants, as shown by the supplementary result using all participants' data (Supplementary Materials, Fig. S2).

To identify other possible factors affecting the response amplitudes, we checked the scalp-cortex distance (SCD) for the COI. The means and SDs were 13.6 ± 2.2 and 17.6 ± 2.6 mm for the WM and TAP tasks, respectively. The SCD for the TAP task (sensorimotor area) was

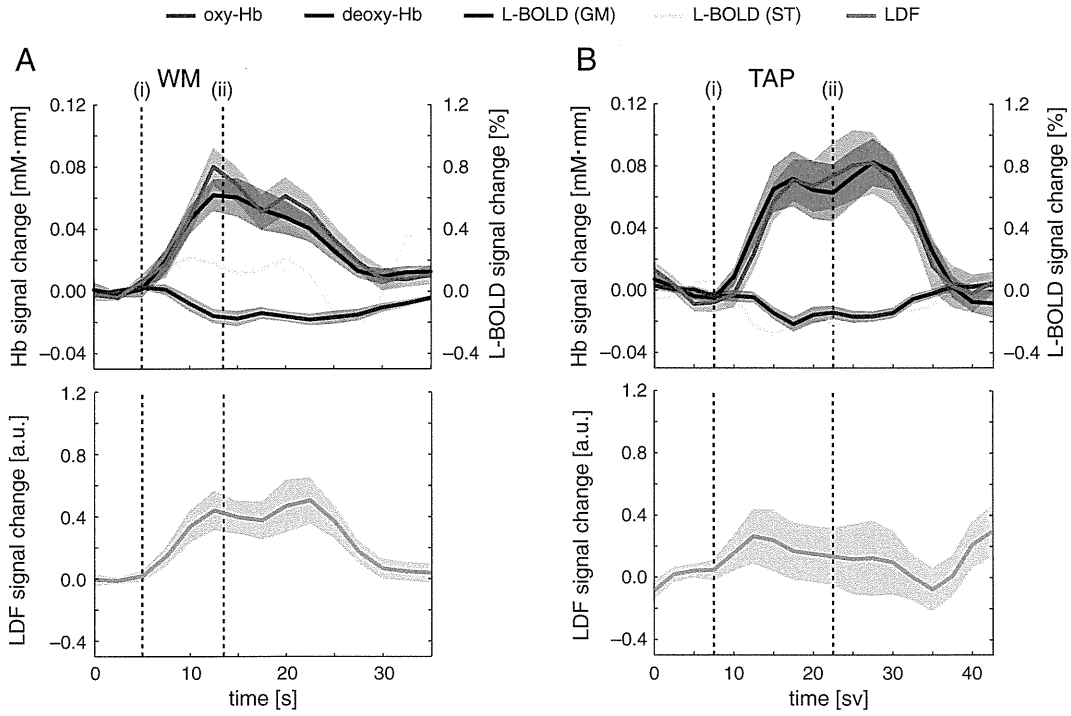

Fig. 7. Block-averaged timecourses of NIRS-Hb, L-BOLD, and LDF signals with standard error (transparent color region) for COI. LDF signals are average of data from two channels. (A) Time courses for WM task (N = 19). (i) Time of Target stimuli (start of encoding), (ii) Time of Test stimuli (end of maintenance and start of retrieval). (B) Time courses for TAP task (N = 16). (i) Time of task start (start cue presented), (ii) Time of task end (end cue presented).

Table 3
Mean ± standard deviation of effect size (d) of NIRS and BOLD signals in COI and LDF signals.

	NIRS		fMRI		LDF
	Oxy-Hb	Deoxy_Hb	L-BOLD (GM)	L-BOLD (ST)	
WM	2.56 ± 1.68	−1.62 ± 1.59	1.83 ± 1.23	0.29 ± 0.96	1.06 ± 1.48
TAP	3.22 ± 3.85	−2.01 ± 2.24	3.65 ± 5.57	−0.26 ± 1.28	0.76 ± 1.52

significantly larger than that for the WM one (PFC) (two-tailed t-test, $p < 5 \times 10^{-5}$). The means and SDs of the SCD for all NIRS channels are listed in the Supplementary Materials (Table S2).

Spatial distribution of temporal correlations of NIRS-Hb signals with L-BOLD and LDF signals

As an additional analysis, we examined the general tendency of the correlation coefficients between the NIRS and L-BOLD (GM) signals for a wide area using the data of Probe-1. The correlation coefficients between the NIRS-Hb and L-BOLD (GM) signals for all NIRS channels are mapped in Fig. 9A and show the spatial distribution. The middle to lower parts of the central area and upper parts of the bilateral ends indicate relatively high correlation coefficients for both tasks. The area dependency of the correlation pattern was examined by grouping the 52 NIRS channels into three areas on the basis of the results of clustering analysis (Fig. 9B). In Area 1 which mainly included BAs 2, 3, 10, 22, 40, and 46, the correlation coefficients between the NIRS-Hb and L-BOLD (GM) signals were significantly different from zero for both tasks. This is in agreement with the results for the activation area (COI). Fifteen NIRS channels adjacent to Area 1 were grouped as Area 2. Although the results for these channels showed a tendency similar to those for the channels in Area 1, the correlation coefficients were lower and statistically significant only for the oxy-Hb signals. In contrast to the results for the NIRS channels in Areas 1 and 2, the results for those in Area 3 (i.e., the ones around the center of the top lines of the NIRS probe holder and the bilateral temple area) showed almost no correlation between the NIRS-Hb and L-BOLD (GM) signals. Regarding the temple area, the distances between the scalp and brain were relatively large (Fig. 10A and Table S1 in Supplementary Materials). Correlation maps for the L-BOLD (ST) and LDF signals are shown (Figs. 10B and C) for comparison with the spatial pattern of the correlation with the L-BOLD (GM) signals. Although there was almost no correlation between the L-BOLD (ST) and NIRS-Hb signals (Fig. 10B), there was relatively large correlation between the LDF and NIRS-Hb signals, mainly around the center of the forehead (Fig. 10C). The spatial patterns of the correlation between the LDF and NIRS-Hb signals did not depend on the position of the LDF, as indicated by the similar maps for channel 1 and channel 2 (Fig. 10C).

Discussion

The present study examined the criterion-related validity of prefrontal NIRS-Hb signals by investigating their similarity with BOLD signals, the gold standard for brain-function measurements. Our use of a relatively reliable task paradigm to measure PFC activation in a large number of participants (N = 27) for simultaneous NIRS, fMRI, and LDF measurements enabled us to partially clarify the nature of the prefrontal NIRS-Hb signals. Statistical analysis demonstrated that prefrontal NIRS-Hb signals in the activation area were significantly correlated with the BOLD signals in the GM rather than those in the ST or skin blood flow measured with the LDF. Moreover, the amplitudes of the task-related responses of the NIRS-Hb signals were significantly correlated with the L-BOLD (GM) signals across participants. These results support the validity of using NIRS to measure hemodynamic signals originating from prefrontal cortical activation; i.e., it is comparable to using BOLD signals measured by fMRI.

Table 4
Mean ± standard deviation of correlation coefficient (r) across participants for block-averaged timecourses in COI.

	WM		TAP	
	Oxy-Hb	Deoxy-Hb	Oxy-Hb	Deoxy-Hb
L-BOLD (GM)	0.69 ± 0.26	−0.50 ± 0.35	0.60 ± 0.33	−0.56 ± 0.33
L-BOLD (ST)	0.22 ± 0.46	−0.04 ± 0.47	−0.14 ± 0.50	0.08 ± 0.48
LDF	0.52 ± 0.46	−0.17 ± 0.39	0.19 ± 0.37	0.01 ± 0.41

Voxel sphere for correlation analysis

To compare the BOLD signals with the NIRS-Hb signals, we first defined a voxel cluster corresponding to each NIRS channel as a sphere for analysis (SFA) on the basis of the photon-path-distribution function (Feng et al., 1995). For each voxel in the GM and ST layers in the SFA, we found that ~50% of the GM voxels were significantly correlated with the NIRS-Hb signals even with a strict threshold, which was corrected for the total number of object voxels (>200, see Table 2). This suggests that the photon-path-distribution function is useful and that the NIRS-Hb signals mainly reflect hemodynamics in GM. About 7–17% of the ST voxels were also significantly correlated with the NIRS-Hb signals, which indicates that the hemodynamics in the superficial layer has an effect to some extent (Firbank et al., 1998; Toronov et al., 2001). However, the correlated voxels were significantly more numerous in the GM region than in the ST region, suggesting that hemodynamic changes in GM make a dominant contribution to NIRS-Hb signals.

For a more in-depth examination of the NIRS–BOLD correlation, we derived the spatially weighted L-BOLD signal from the SFA (Sassaroli et al., 2006) as a representative temporal BOLD signal. Compared to a conventional method in which the projection point is identified on the brain surface from the midpoint between the source and detector on the scalp (Cui et al., 2011; Sasai et al., 2012), the present approach is advantageous because it takes into account the spatial dependence of the BOLD signals on the NIRS-Hb signal (Sassaroli et al., 2006). As more complex simulations using anatomical information come to be used to define voxel clusters for individual NIRS channels (Haeussinger et al., 2011; Heinzel et al., 2013), more methods for obtaining suitable BOLD signals will be developed. Nonetheless, our results and those in a previous study (Sassaroli et al., 2006) demonstrate that the present approach is useful for a quantitative comparison of NIRS and BOLD signals.

Temporal correlation of NIRS and L-BOLD signals in activation area

The results of our temporal correlation analysis between the L-BOLD (GM) and NIRS-Hb signals in the activation area showed significant correlation, a finding basically in agreement with those of previous studies (Cui et al., 2011; Heinzel et al., 2013; Mehagnoul-Schipper et al., 2002; Sassaroli et al., 2006; Strangman et al., 2002). Most previous NIRS–fMRI studies have used primary visual and/or motor tasks, which could induce a relatively reliable cortical activation, and showed a high correlation between the two modality signals. In contrast, only a few NIRS–fMRI studies have examined activation signals in the PFC. In a recent representative study (Cui et al., 2011), both the prefrontal and parietal regions were measured using a battery of cognitive tasks including finger tapping and N-back WM tasks. A comparison using the mean BOLD–NIRS correlation for all NIRS channels over a wide area of the PFC and parietal cortex revealed NIRS–BOLD correlation for both the cognitive and finger tapping tasks. However, as the strength of the correlation can be affected by whether or not the area is activated by the task, there

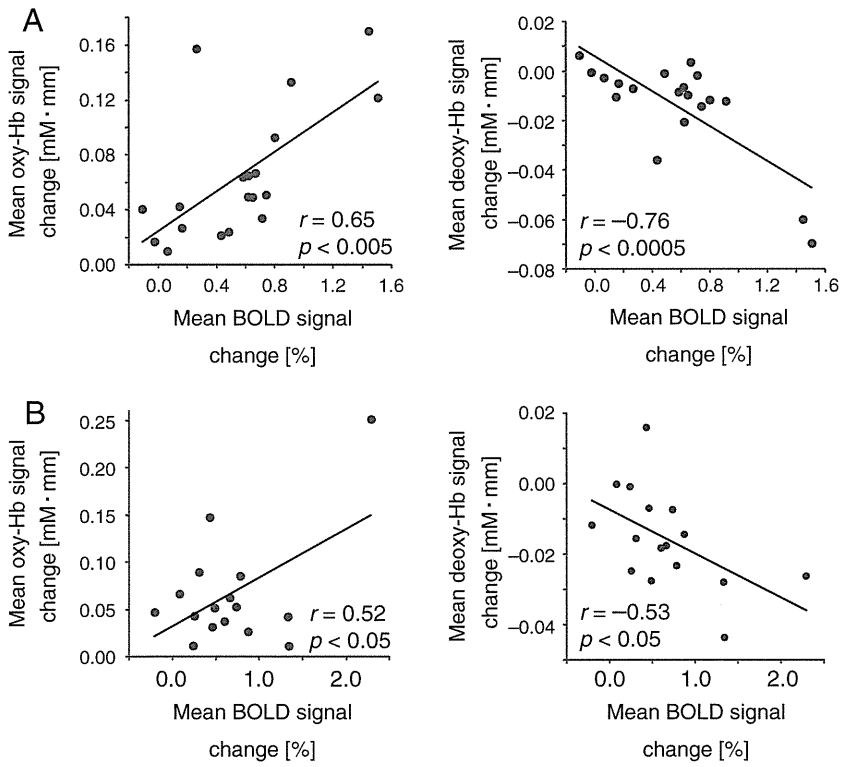

Fig. 8. Correlation between mean changes in NIRS-Hb signals and those in L-BOLD signals. Red dots indicate NIRS oxy-Hb signal and blue dots indicate NIRS deoxy-Hb signal: (A) PFC during WM task; (B) sensorimotor cortex during TAP task.

should first be a comparison of the correlation for a specified activation area known to be involved in each task. Accordingly, we compared the NIRS-Hb and L-BOLD (GM) signals for the PFC for the WM task and for the sensorimotor area for the TAP task. We found that there was correlation for both the continuous data (mean $|r| =$ 0.38–0.59, Fig. 6) and for the block-averaged data (mean $|r| =$ 0.50–0.69, Table 4) for both tasks. Our finding of correlation higher than that reported by Cui et al. (2011) (mean $|r| = 0.20$–0.25 for each task) adds more specific information on the temporal correlation between NIRS and BOLD signals to the literature.

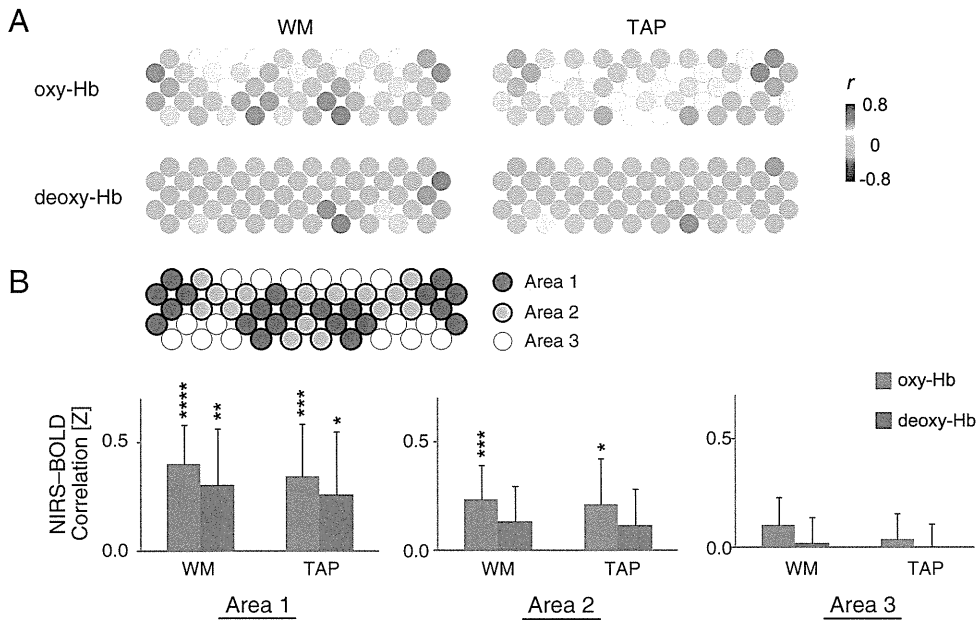

Fig. 9. Spatial distribution of correlation coefficients between NIRS-Hb and L-BOLD (GM) signals for Probe-1 data. (A) Correlation between NIRS-Hb and L-BOLD (GM) signals in WM and TAP tasks. (B) Correlation between NIRS-Hb and L-BOLD (GM) signals in three areas determined by clustering analysis using spatial pattern of correlation maps in (A). In bar graphs, mean and standard deviation of correlation coefficients (Z-values) between NIRS and L-BOLD signals in NIRS channels for each area are shown for WM and TAP tasks. Sign of correlation coefficients for NIRS deoxy-Hb was inverted for comparison with results for NIRS oxy-Hb signals. Statistical significance against zero is shown ($^{****}p < 10^{-5}$, $^{***}p < \times 10^{-3}$, $^{**}p < 10^{-2}$, $^{*}p < 5 \times 10^{-2}$).

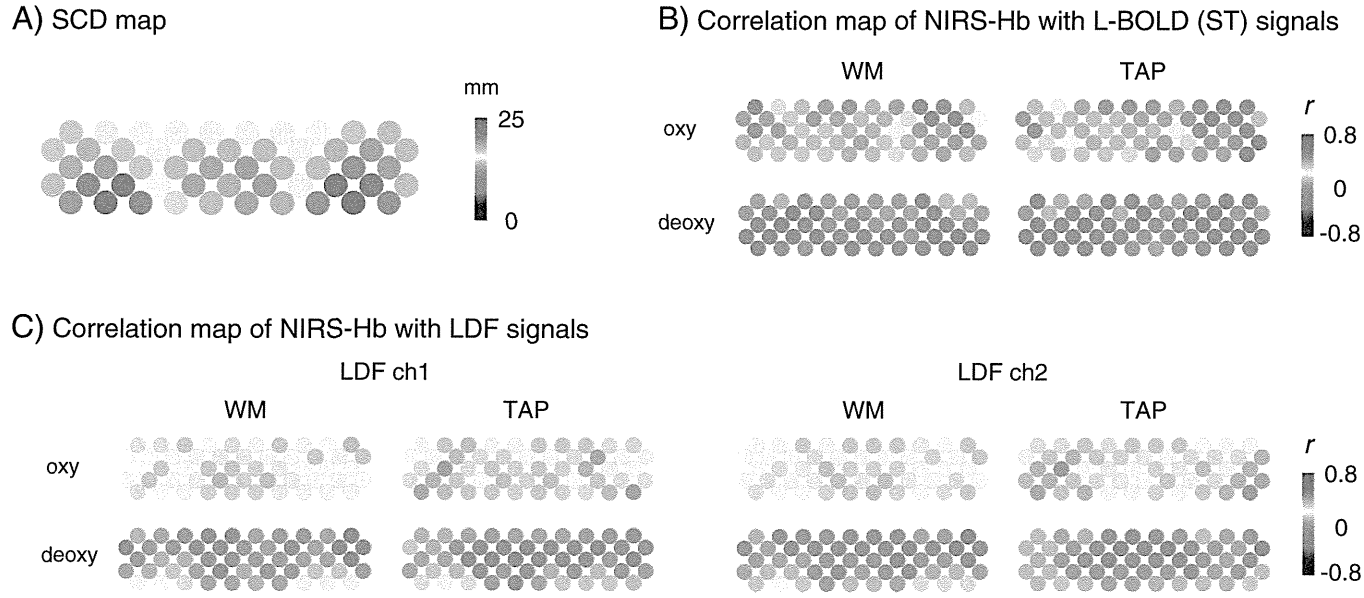

Fig. 10. Spatial distribution of potential factors affecting correlation coefficients between NIRS-Hb and BOLD signals. (A) Mean scalp-cortex distance (SCD) across 15 participants (Probe-1). Raw numerical data are shown in Supplementary Materials (Table S2). (B) Maps of correlation coefficients between NIRS-Hb and L-BOLD (ST) signals. (C) Maps of correlation coefficients between NIRS-Hb and LDF signals. LDF results for channel 1 (center point between eyebrows) are shown in the left and LDF results for channel 2 (around left temple) are shown in the right.

Amplitude correlation of NIRS and BOLD activation signals

An important finding of our study is a significant correlation between NIRS-Hb and BOLD signals in the response amplitude. This correlation was particularly evident in the PFC responses for the WM task, in which participants with a stronger NIRS-Hb response showed a stronger L-BOLD (GM) response (oxy-Hb: $r = 0.65$, deoxy-Hb: $r = -0.76$). This is the first report of amplitude correlation between NIRS-Hb and BOLD signals in the PFC, as far as we know. A similar correlation was reported for sensorimotor activation (Mehagnoul-Schipper et al., 2002). Given that the unit for the NIRS-Hb signals is the product of the change in the Hb concentration (mM) and the effective optical path length (mm), we consider that this finding demonstrates that the variation in the effective optical path length is small enough for NIRS-Hb signals to be obtained that reflect individual differences in functional activity. However, the generality of this tendency is not clear because the SCDs are variable among NIRS channels (Supplementary Material, Table S2) while the SCD in the activation area for the WM task was relatively small (13.6 ± 2.15 mm). Indeed, in the COI for the TAP task, the amplitude correlation was lower (oxy-Hb: $r = 0.52$; deoxy-Hb: $r = -0.53$) and the SCD was longer (17.6 ± 2.62 mm) than for the WM task. Although other factors such as the presence of hair should be considered for a more generalized conclusion, our results suggest that the NIRS-Hb signal amplitude for a WM task around BA46 at least reflects comparable hemodynamic information in fMRI measurements.

Effect of superficial hemodynamics on NIRS-Hb signals

We used L-BOLD signals in soft tissue regions and LDF signals as data representing extracranial hemodynamic changes to investigate the effect of superficial hemodynamics on NIRS-Hb signals. Kirilina et al. (2012) used NIRS to measure a task-related systemic signal similar to the extracranial BOLD signal of forehead veins. However, the task-related change they used was not a conventional hemodynamic response; it peaked a few seconds after task onset and linearly decreased until a few seconds after the end of the task. This change is similar to the piece-wise task-related component observed by Katura et al. (2008) and Tanaka et al. (2013). We did not observe such an uncommon pattern of NIRS-Hb signals in the activation area, probably because the conventional hemodynamic change was dominant in the proven functional areas. This pattern might be evident if a task paradigm inducing a strong systemic change is used (Kirilina et al., 2012) or if a signal-processing method that separates signal components is used (Katura et al., 2008; Tanaka et al., 2013). Although there were different sensitivities for the BOLD (GM) and BOLD (ST) signals (the intensity of the BOLD signals in GM was about 100 times that in ST, the present study nevertheless demonstrated that NIRS-Hb signals are significantly correlated with L-BOLD (GM) ones and not with L-BOLD (ST) ones. It thus provided supportive evidence that NIRS can be used to measure hemodynamic signals originating from cortical activation.

However, the LDF signals showed a time-locked increase for the WM task and a significant temporal correlation with the NIRS oxy-Hb signals in the prefrontal region. The correlation was not significant for the deoxy-Hb signals or for any of the signals in the sensorimotor area for the TAP task. This suggests that skin blood flow in the forehead increases following the WM task, which mainly affects the prefrontal oxy-Hb signals to some extent. Previous studies consistently found that the effect of systemic signals is relatively dominant in the oxy-Hb signal (Franceschini et al., 2003; Funane et al., 2013; Kirilina et al., 2012). As the amplitudes of the NIRS deoxy-Hb responses were more clearly correlated with the L-BOLD (GM) responses than were those of the NIRS oxy-Hb responses (Fig. 8A), it is possible that the NIRS deoxy-Hb signal reflected the brain signal more accurately than the oxy-Hb signal did. This might explain why a NIRS study investigating PFC activity found a robust effect supporting their conclusion only in the deoxy-Hb signal (Heilbronner and Munte, 2013).

Although additional research is needed to determine the effect of skin blood flow measured by LDF, our results demonstrated that the temporal correlation between NIRS-Hb and L-BOLD (GM) signals is significantly stronger than that between NIRS-Hb and LDF signals. Moreover, we found a correlation between the amplitudes of the NIRS-Hb and L-BOLD (GM) signals. Given these findings, we conclude that the effect of the skin blood flow is negligible in the evaluation of task-related activation, at least in BA 46, for this WM task. The

expected development of a method for separating the superficial signals from the deep brain signals will enable us to obtain NIRS-Hb signals that are less affected by skin blood flow during the performance of a wide range of tasks (Funane et al., 2013).

Spatial variability of NIRS–BOLD correlation

Correlation analysis was conducted for each NIRS channel to determine the spatial variability of the NIRS–BOLD correlations (Fig. 9). The regions in the middle of the PFC and around the sensorimotor cortices (including the inferior parietal cortex and the superior temporal cortex) showed higher correlation coefficients for both tasks. The correlation maps agree with the findings of a previous study (Cui et al., 2011), which found that the spatial pattern of the NIRS–BOLD correlations were similar across four different tasks. These results suggest that NIRS–BOLD correlation depends on the anatomical characteristics of the region as well as the task paradigm. Indeed, previous studies (Cui et al., 2011; Heinzel et al., 2013) have shown that the SCD, the GM volume penetrated by light, and the CNR contribute to the strength of the temporal correlation between the NIRS-Hb and BOLD signals. These results are reasonable given that it is natural that a larger SCD or smaller GM volume would cause lower sensitivity for cortical signals with larger noise and that a higher noise level can reduce the correlation coefficients.

Our data show that the NIRS-Hb signals in the channels in the middle of the top line and those around the bilateral temple area had almost no correlation with the BOLD signals in the GM (Fig. 9B). The larger noise level for the signals in the channels in the middle of the top line due to hair might explain their lack of correlation. The lower correlation for the NIRS-Hb signals in the channels in the temple area may have been due to an anatomical feature, such as a longer SCD (see Fig. 10A). Furthermore, the lack of correlation might be the result of a more complex phenomenon as a few previous studies have indicated that NIRS-Hb signals around the temple area are uniquely correlated with the extracranial BOLD signals (Heinzel et al., 2013; Sasai et al., 2012; Sato et al., 2011b). Although the present study did not reveal a high correlation between the L-BOLD (ST) and NIRS-Hb signals, the target frequency for the analysis might explain the difference in findings from the previous studies. The present study focused on task-related signals higher than 0.0125 Hz or 0.0150 Hz for the high-pass filtering while the previous studies focused on a lower frequency such as 0.0078 Hz (Heinzel et al., 2013), 0.0090 Hz (Sasai et al., 2012), and 0.0034 Hz (Sato et al., 2011b).

In addition, we found high temporal correlation between the LDF and NIRS oxy-Hb signals in the middle of the prefrontal region. The spatial distribution for the high correlation area was not particularly localized regardless of the LDF measurement position (Fig. 10C). This result is in agreement with those of previous studies (Aletti et al., 2012; Kohno et al., 2007) and indicates that the skin blood flow, which is measured with an LDF, affects oxy-Hb signals in a wide region of the forehead. Thus, our results indicate that there is different spatial variability between the L-BOLD (ST) and LDF signals in relation to the NIRS-Hb signals (Fig. 10). This suggests that L-BOLD (ST) signals are not sensitive to superficial skin blood flow, which can be measured with an LDF.

Limitations and future perspective

Several limitations of our study should be borne in mind. First, we took a NIRS-based approach, with our main analysis focused on the activation area determined by the NIRS-Hb signals. This approach is good for examining whether a type 1 error (false positive) occurs in the prefrontal NIRS-Hb signals but not for a type 2 error (false negative) in which NIRS fails to detect a true cortical activation. An integrated approach is needed for more precise validation of NIRS-Hb signals for functional measurements. Second, BOLD (ST) signals have a lower intensity than BOLD (GM) ones. Although previous studies have suggested the usefulness of BOLD (ST) signals for examining task-evoked extracranial signals (Heinzel et al., 2013; Kirilina et al., 2012) and our results demonstrate that NIRS-Hb signals are correlated with the BOLD (GM) signals rather than the BOLD (ST) ones, a detailed examination of the characteristics of BOLD (ST) signals is needed. Third, we examined activation signals for tasks with standard durations (~15 s), which limited us to a certain frequency band (>0.0125 Hz). We suggested that the correlation between BOLD (ST) and NIRS-Hb signals depends on the target frequency band, and the use of BOLD (ST) signals at lower frequencies (<0.01 Hz) is an issue needing to be explored. In addition, the posture of participants might be another factor influencing the effects of skin blood flow during a task. The simultaneous NIRS and fMRI measurements were performed in the supine position while normal NIRS measurements are performed in the sitting position. As a previous study reported a significant effect of head-of-bed positioning on frontal NIRS signals (Durduran et al., 2009), the effect of participant position needs to be determined.

Taking a future perspective, we see a need to clarify the factors affecting the correlation between NIRS-Hb and BOLD signals. The effect of such factors as SCD, CNR, and GM volume (Cui et al., 2011; Heinzel et al., 2013) are intertwined, making it difficult to isolate their effects by using a simple correlation analysis. There is also a need to use the simultaneous NIRS–fMRI data to validate a newly proposed method for removing the superficial hemodynamic effects (Funane et al., 2013).

Conclusion

We conducted simultaneous NIRS, fMRI, and LDF measurements to determine whether prefrontal NIRS-Hb signals reflect cortical activity rather than superficial effects. Correlation analysis demonstrated that NIRS-Hb signals in the PFC activation area are significantly correlated with BOLD signals in gray matter rather than with such signals in soft tissue or LDF signals. Moreover, the amplitudes of the task-related responses of the NIRS-Hb signals were significantly correlated with those of the L-BOLD (GM) signals across participants. These results provide supportive evidence for the validity of prefrontal NIRS-Hb signals, meaning that the NIRS-Hb signal is comparable to the BOLD signal measured by fMRI.

Acknowledgments

We thank Mr. Tsuyoshi Miyashita, Dr. Hirokazu Tanaka, and Dr. Eisuke Sakakibara for their assistance with the experiments, Dr. Daisuke Suzuki, Mr. Michiyuki Fujiwara, and Mr. Shingo Kawasaki for providing technical assistance, and Dr. Akiko Obata and Dr. Ryuta Aoki for their helpful comments on the experimental design. This study was supported by Grants-in-Aid for Scientific Research on Innovative Areas (nos. 23118001 & 23118004 [Adolescent Mind & Self-Regulation] to KK, no. 32118003 to MF, and Comprehensive Brain Science Network to KK), a Grant-in-Aid for Young Scientists (B) (no. 23791309) to RT, a Grant-in-Aid for Scientific Research (B) (no. 23390286) to MF, and a Grant-in-Aid for Challenging Exploratory Research (no. 22659209) to MF from the Ministry of Education, Culture, Sports, Science and Technology of Japan (MEXT). A part of this study was also the result of the "Development of biomarker candidates for social behavior" interdisciplinary project carried out under the Strategic Research Program for Brain Sciences by MEXT. This study was also supported in part by Health and Labor Sciences Research Grants for Comprehensive Research on Disability Health and Welfare (H23-seishin-ippan-002) to RT, YN, and MF.

Conflict of interest

Hitachi Medical Corporation provided a material support (temporary rental of a NIRS (Optical Topography) ETG-4000 system) for this study.

Appendix A. Supplementary data

Supplementary data to this article can be found online at http://dx.doi.org/10.1016/j.neuroimage.2013.06.043.

References

Aletti, F., Re, R., Pace, V., Contini, D., Molteni, E., Cerutti, S., Maria Bianchi, A., Torricelli, A., Spinelli, L., Cubeddu, R., Baselli, G., 2012. Deep and surface hemodynamic signal from functional time resolved transcranial near infrared spectroscopy compared to skin flowmotion. Comput. Biol. Med. 42, 282–289.

Aoki, R., Sato, H., Katura, T., Utsugi, K., Koizumi, H., Matsuda, R., Maki, A., 2011. Relationship of negative mood with prefrontal cortex activity during working memory tasks: an optical topography study. Neurosci. Res. 70, 189–196.

Aoki, R., Sato, H., Katura, T., Matsuda, R., Koizumi, H., 2013. Correlation between prefrontal cortex activity during working memory tasks and natural mood independent of personality effects: an optical topography study. Psychiatry Res. 212, 79–87.

Atsumori, H., Kiguchi, M., Katura, T., Funane, T., Obata, A., Sato, H., Manaka, T., Iwamoto, M., Maki, A., Koizumi, H., Kubota, K., 2010. Noninvasive imaging of prefrontal activation during attention-demanding tasks performed while walking using a wearable optical topography system. J. Biomed. Opt. 15, 046002.

Buxton, R.B., Uludag, K., Dubowitz, D.J., Liu, T.T., 2004. Modeling the hemodynamic response to brain activation. NeuroImage 23, S220–S233.

Chance, B., Zhuang, Z., UnAh, C., Alter, C., Lipton, L., 1993. Cognition-activated low-frequency modulation of light absorption in human brain. Proc. Natl. Acad. Sci. U. S. A. 90, 3770–3774.

Cohen, J., 1992. A power primer. Psychol. Bull. 112, 155–159.

Cui, X., Bray, S., Bryant, D.M., Glover, G.H., Reiss, A.L., 2011. A quantitative comparison of NIRS and fMRI across multiple cognitive tasks. NeuroImage 54, 2808–2821.

Cui, X., Bryant, D.M., Reiss, A.L., 2012. NIRS-based hyperscanning reveals increased interpersonal coherence in superior frontal cortex during cooperation. NeuroImage 59, 2430–2437.

Delpy, D.T., Cope, M., van der Zee, P., Arridge, S., Wray, S., Wyatt, J., 1988. Estimation of optical pathlength through tissue from direct time of flight measurement. Phys. Med. Biol. 33, 1433–1442.

D'Esposito, M., 2007. From cognitive to neural models of working memory. Philos. Trans. R. Soc. Lond. B Biol. Sci. 362, 761–772.

Durduran, T., Zhou, C., Edlow, B.L., Yu, G., Choe, R., Kim, M.N., Cucchiara, B.L., Putt, M.E., Shah, Q., Kasner, S.E., Greenberg, J.H., Yodh, A.G., Detre, J.A., 2009. Transcranial optical monitoring of cerebrovascular hemodynamics in acute stroke patients. Opt. Express 17, 3884–3902.

Feng, S., Zeng, F.A., Chance, B., 1995. Photon migration in the presence of a single defect: a perturbation analysis. Appl. Opt. 34, 3826–3837.

Firbank, M., Okada, E., Delpy, D.T., 1998. A theoretical study of the signal contribution of regions of the adult head to near-infrared spectroscopy studies of visual evoked responses. NeuroImage 8, 69–78.

Fisher, R.A., 1915. Frequency distribution of the values of the correlation coefficient in samples from an indefinitely large population. Biometrika 10, 507–521.

Fisher, R.A., 1921. On the "probable error" of a coefficient of correlation deduced from a small sample. Metron 1, 3–32.

Franceschini, M.A., Fantini, S., Thompson, J.H., Culver, J.P., Boas, D.A., 2003. Hemodynamic evoked response of the sensorimotor cortex measured noninvasively with near-infrared optical imaging. Psychophysiology 40, 548–560.

Funane, T., Kiguchi, M., Atsumori, H., Sato, H., Kubota, K., Koizumi, H., 2011. Synchronous activity of two people's prefrontal cortices during a cooperative task measured by simultaneous near-infrared spectroscopy. J. Biomed. Opt. 16, 077011.

Funane, T., Atsumori, H., Katura, T., Obata, A.N., Sato, H., Tanikawa, Y., Okada, E., Kiguchi, M., 2013. Quantitative evaluation of deep and shallow tissue layers' contribution to fNIRS signal using multi-distance optodes and independent component analysis. NeuroImage. http://dx.doi.org/10.1016/j.neuroimage.2013.02.026.

Genovese, C.R., Lazar, N.A., Nichols, T., 2002. Thresholding of statistical maps in functional neuroimaging using the false discovery rate. NeuroImage 15, 870–878.

Germon, T.J., Kane, N.M., Manara, A.R., Nelson, R.J., 1994. Near-infrared spectroscopy in adults: effects of extracranial ischaemia and intracranial hypoxia on estimation of cerebral oxygenation. Br. J. Anaesth. 73, 503–506.

Germon, T.J., Evans, P.D., Manara, A.R., Barnett, N.J., Wall, P., Nelson, R.J., 1998. Sensitivity of near infrared spectroscopy to cerebral and extra-cerebral oxygenation changes is determined by emitter-detector separation. J. Clin. Monit. Comput. 14, 353–360.

Goldman-Rakic, P.S., 1987. Circuitry of primate prefrontal cortex and regulation of behavior by representational memory. In: Plum, F. (Ed.), Handbook of Physiology. The Nervous System. Higher Functions of the Brain. American Physiological Society, Bethesda, MD.

Haeussinger, F.B., Heinzel, S., Hahn, T., Schecklmann, M., Ehlis, A.C., Fallgatter, A.J., 2011. Simulation of near-infrared light absorption considering individual head and prefrontal cortex anatomy: implications for optical neuroimaging. PLoS One 6, e26377.

Heilbronner, U., Munte, T.F., 2013. Rapid event-related near-infrared spectroscopy detects age-related qualitative changes in the neural correlates of response inhibition. NeuroImage 65, 408–415.

Heinzel, S., Haeussinger, F.B., Hahn, T., Ehlis, A.C., Plichta, M.M., Fallgatter, A.J., 2013. Variability of (functional) hemodynamics as measured with simultaneous fNIRS and fMRI during intertemporal choice. NeuroImage 71, 125–134.

Homae, F., Watanabe, H., Otobe, T., Nakano, T., Go, T., Konishi, Y., Taga, G., 2010. Development of global cortical networks in early infancy. J. Neurosci. 30, 4877–4882.

Hoshi, Y., Tamura, M., 1993. Detection of dynamic changes in cerebral oxygenation coupled to neuronal function during mental work in man. Neurosci. Lett. 150, 5–8.

Huppert, T.J., Hoge, R.D., Diamond, S.G., Franceschini, M.A., Boas, D.A., 2006. A temporal comparison of BOLD, ASL, and NIRS hemodynamic responses to motor stimuli in adult humans. NeuroImage 29, 368–382.

Jöbsis, F.F., 1977. Noninvasive, infrared monitoring of cerebral and myocardial oxygen sufficiency and circulatory parameters. Science 198, 1264–1267.

Jöbsis-VanderVliet, F.F., Piantadosi, C.A., Sylvia, A.L., Lucas, S.K., Keizer, H.H., 1988. Near-infrared monitoring of cerebral oxygen sufficiency. I. Spectra of cytochrome c oxidase. Neurol. Res. 10, 7–17.

Kato, T., Kamei, A., Takashima, S., Ozaki, T., 1993. Human visual cortical function during photic stimulation monitoring by means of near-infrared spectroscopy. J. Cereb. Blood Flow Metab. 13, 516–520.

Katura, T., Sato, H., Fuchino, Y., Yoshida, T., Atsumori, H., Kiguchi, M., Maki, A., Abe, M., Tanaka, N., 2008. Extracting task-related activation components from optical topography measurement using independent components analysis. J. Biomed. Opt. 13, 054008.

Kirilina, E., Jelzow, A., Heine, A., Niessing, M., Wabnitz, H., Bruhl, R., Ittermann, B., Jacobs, A.M., Tachtsidis, I., 2012. The physiological origin of task-evoked systemic artefacts in functional near infrared spectroscopy. NeuroImage 61, 70–81.

Kleinschmidt, A., Obrig, H., Requardt, M., Merboldt, K.D., Dirnagl, U., Villringer, A., Frahm, J., 1996. Simultaneous recording of cerebral blood oxygenation changes during human brain activation by magnetic resonance imaging and near-infrared spectroscopy. J. Cereb. Blood Flow Metab. 16, 817–826.

Kohno, S., Miyai, I., Seiyama, A., Oda, I., Ishikawa, A., Tsuneishi, S., Amita, T., Shimizu, K., 2007. Removal of the skin blood flow artifact in functional near-infrared spectroscopic imaging data through independent component analysis. J. Biomed. Opt. 12, 062111.

Kubota, K., Niki, H., 1971. Prefrontal cortical unit activity and delayed alternation performance in monkeys. J. Neurophysiol. 34, 337–347.

Maki, A., Yamashita, Y., Ito, Y., Watanabe, E., Mayanagi, Y., Koizumi, H., 1995. Spatial and temporal analysis of human motor activity using noninvasive NIR topography. Med. Phys. 22, 1997–2005.

McCarthy, G., Blamire, A.M., Puce, A., Nobre, A.C., Bloch, G., Hyder, F., Goldman-Rakic, P., Shulman, R.G., 1994. Functional magnetic resonance imaging of human prefrontal cortex activation during a spatial working memory task. Proc. Natl. Acad. Sci. U. S. A. 91, 8690–8694.

McCarthy, G., Puce, A., Constable, R.T., Krystal, J.H., Gore, J.C., Goldman-Rakic, P., 1996. Activation of human prefrontal cortex during spatial and nonspatial working memory tasks measured by functional MRI. Cereb. Cortex 6, 600–611.

Mehagnoul-Schipper, D.J., van der Kallen, B.F., Colier, W.N., van der Sluijs, M.C., van Erning, L.J., Thijssen, H.O., Oeseburg, B., Hoefnagels, W.H., Jansen, R.W., 2002. Simultaneous measurements of cerebral oxygenation changes during brain activation by near-infrared spectroscopy and functional magnetic resonance imaging in healthy young and elderly subjects. Hum. Brain Mapp. 16, 14–23.

Millikan, G.A., 1942. The oxymeter, an instrument for measuring continuously the oxygen saturation of arterial blood in man. Rev. Sci. Instrum. 13, 434–444.

Minagawa-Kawai, Y., van der Lely, H., Ramus, F., Sato, Y., Mazuka, R., Dupoux, E., 2011. Optical brain imaging reveals general auditory and language-specific processing in early infant development. Cereb. Cortex 21, 254–261.

Miyai, I., Tanabe, H.C., Sase, I., Eda, H., Oda, I., Konishi, I., Tsunazawa, Y., Suzuki, T., Yanagida, T., Kubota, K., 2001. Cortical mapping of gait in humans: a near-infrared spectroscopic topography study. NeuroImage 14, 1186–1192.

Ogawa, S., Lee, T.M., Kay, A.R., Tank, D.W., 1990a. Brain magnetic resonance imaging with contrast dependent on blood oxygenation. Proc. Natl. Acad. Sci. U. S. A. 87, 9868–9872.

Ogawa, S., Lee, T.M., Nayak, A.S., Glynn, P., 1990b. Oxygenation-sensitive contrast in magnetic resonance image of rodent brain at high magnetic fields. Magn. Reson. Med. 14, 68–78.

Pena, M., Maki, A., Kovacic, D., Dehaene-Lambertz, G., Koizumi, H., Bouquet, F., Mehler, J., 2003. Sounds and silence: an optical topography study of language recognition at birth. Proc. Natl. Acad. Sci. U. S. A. 100, 11702–11705.

Rorden, C., Brett, M., 2000. Stereotaxic display of brain lesions. Behav. Neurol. 12, 191–200.

Sasai, S., Homae, F., Watanabe, H., Sasaki, A.T., Tanabe, H.C., Sadato, N., Taga, G., 2012. A NIRS–fMRI study of resting state network. NeuroImage 63, 179–193.

Sassaroli, A., de, B.F.B., Tong, Y., Renshaw, P.F., Fantini, S., 2006. Spatially weighted BOLD signal for comparison of functional magnetic resonance imaging and near-infrared imaging of the brain. NeuroImage 33, 505–514.

Sato, H., Fuchino, Y., Kiguchi, M., Katura, T., Maki, A., Yoro, T., Koizumi, H., 2005. Intersubject variability of near-infrared spectroscopy signals during sensorimotor cortex activation. J. Biomed. Opt. 10, 044001.

Sato, H., Kiguchi, M., Maki, A., Fuchino, Y., Obata, A., Yoro, T., Koizumi, H., 2006. Within-subject reproducibility of near-infrared spectroscopy signals in sensorimotor activation after 6 months. J. Biomed. Opt. 11, 014021.

Sato, H., Aoki, R., Katura, T., Matsuda, R., Koizumi, H., 2011a. Correlation of within-individual fluctuation of depressed mood with prefrontal cortex activity during verbal working memory task: optical topography study. J. Biomed. Opt. 16, 126007.

Sato, H., Obata, A.N., Moda, I., Ozaki, K., Yasuhara, T., Yamamoto, Y., Kiguchi, M., Maki, A., Kubota, K., Koizumi, H., 2011b. Application of near-infrared spectroscopy to measurement of hemodynamic signals accompanying stimulated saliva secretion. J. Biomed. Opt. 16, 047002.

Sato, H., Hirabayashi, Y., Tsubokura, H., Kanai, M., Ashida, T., Konishi, I., Uchida-Ota, M., Konishi, Y., Maki, A., 2012. Cerebral hemodynamics in newborn infants exposed to speech sounds: a whole-head optical topography study. Hum. Brain Mapp. 33, 2092–2103.

Strangman, G., Culver, J.P., Thompson, J.H., Boas, D.A., 2002. A quantitative comparison of simultaneous BOLD fMRI and NIRS recordings during functional brain activation. NeuroImage 17, 719–731.

Taga, G., Asakawa, K., Maki, A., Konishi, Y., Koizumi, H., 2003. Brain imaging in awake infants by near-infrared optical topography. Proc. Natl. Acad. Sci. U. S. A. 100, 10722–10727.

Takahashi, T., Takikawa, Y., Kawagoe, R., Shibuya, S., Iwano, T., Kitazawa, S., 2011. Influence of skin blood flow on near-infrared spectroscopy signals measured on the forehead during a verbal fluency task. NeuroImage 57, 991–1002.

Tanaka, H., Katura, T., Sato, H., 2013. Task-related component analysis for functional neuroimaging and application to near-infrared spectroscopy data. NeuroImage 64, 308–327.

Toronov, V., Webb, A., Choi, J.H., Wolf, M., Michalos, A., Gratton, E., Hueber, D., 2001. Investigation of human brain hemodynamics by simultaneous near-infrared spectroscopy and functional magnetic resonance imaging. Med. Phys. 28, 521–527.

Toronov, V., Walker, S., Gupta, R., Choi, J.H., Gratton, E., Hueber, D., Webb, A., 2003. The roles of changes in deoxyhemoglobin concentration and regional cerebral blood volume in the fMRI BOLD signal. NeuroImage 19, 1521–1531.

Tsujimoto, S., Postle, B.R., 2012. The prefrontal cortex and oculomotor delayed response: a reconsideration of the "mnemonic scotoma". J. Cogn. Neurosci. 24, 627–635.

Tsujimoto, S., Yamamoto, T., Kawaguchi, H., Koizumi, H., Sawaguchi, T., 2004. Prefrontal cortical activation associated with working memory in adults and preschool children: an event-related optical topography study. Cereb. Cortex 14, 703–712.

Villringer, A., Planck, J., Hock, C., Schleinkofer, L., Dirnagl, U., 1993. Near infrared spectroscopy (NIRS): a new tool to study hemodynamic changes during activation of brain function in human adults. Neurosci. Lett. 154, 101–104.

Wray, S., Cope, M., Delpy, D.T., Wyatt, J.S., 1988. Characterization of the near infrared absorption spectra of cytochrome aa3 and haemoglobin for the non-invasive monitoring of cerebral oxygenation. Biochim. Biophys. Acta 933, 184–192.

Yamashita, Y., Maki, A., Ito, Y., Watanabe, E., Mayanagi, H., Koizumi, H., 1996. Noninvasive near-infrared topography of human brain activity using intensity modulation spectroscopy. Opt. Eng. 35, 1046–1049.

Schizophrenia Research 150 (2013) 459–467

Contents lists available at ScienceDirect

Schizophrenia Research

journal homepage: www.elsevier.com/locate/schres

Differential spatiotemporal characteristics of the prefrontal hemodynamic response and their association with functional impairment in schizophrenia and major depression

Masaru Kinou [a,1], Ryu Takizawa [a,b,*,1], Kohei Marumo [a], Shingo Kawasaki [a,c], Yuki Kawakubo [d], Masato Fukuda [e], Kiyoto Kasai [a]

[a] Department of Neuropsychiatry, Graduate School of Medicine, The University of Tokyo, 7-3-1 Hongo, Bunkyo-ku, Tokyo 113-8655, Japan
[b] MRC Social, Genetic and Developmental Psychiatry Centre, Institute of Psychiatry, King's College London, P080 De Crespigny Park, Denmark Hill, London SE5 8AF, United Kingdom
[c] Optical Topography Group, Application Development Office, Hitachi Medical Corporation, Shintoyofuta 2-1, Kashiwa, Chiba 277-0804, Japan
[d] Department of Child Neuropsychiatry, Graduate School of Medicine, The University of Tokyo, 7-3-1 Hongo, Bunkyo-ku, Tokyo 113-8655, Japan
[e] Department of Psychiatry and Human Behavior, Gunma University Graduate School of Medicine, 3-39-22 Showa-machi, Maebashi, Gunma 371-8511, Japan

ARTICLE INFO

Article history:
Received 15 April 2013
Received in revised form 9 August 2013
Accepted 19 August 2013
Available online 7 September 2013

Keywords:
Schizophrenia
Major depressive disorder
Near-infrared spectroscopy
Prefrontal cortex
Verbal fluency task
Global Assessment of Functioning

ABSTRACT

Recent neuroimaging studies have shown similarities and differences in prefrontal abnormalities between patients with schizophrenia (SZ) and major depressive disorder (MDD). However, the differential spatiotemporal characteristics of these abnormalities and their association with functional impairment remain unclear. To elucidate differential brain pathophysiology in these disorders, we used multichannel near-infrared spectroscopy (NIRS) to measure the spatiotemporal characteristics of prefrontal activation and investigated their association with global functioning levels. The study included 96 individuals: 32 patients with SZ, 32 patients with MDD, and 32 demographically matched healthy subjects. During a verbal fluency task, the changes in oxygenated and deoxygenated hemoglobin ([oxy-Hb] and [deoxy-Hb]) signals over the prefrontal cortex (PFC) were measured using 52-channel NIRS and compared among the 3 groups. Patients with SZ and MDD showed lesser-than-normal [oxy-Hb] activation during the task, whereas the initial slope of [oxy-Hb] activation was steeper for patients with MDD than for patients with SZ. The reduced hemodynamic response was associated with lower global functioning, and the correlative regions were different between the 2 disorders (frontopolar PFC in SZ; dorsolateral and ventrolateral PFC in MDD). The hypofrontality observed in patients with SZ and MDD is consistent with the findings of previous neuroimaging studies. Moreover, the spatiotemporal characteristics and the functional significance of the prefrontal hemodynamic response could differentiate the 2 psychiatric disorders. These results suggest a differential brain pathophysiology between SZ and MDD. Future large-scale studies are needed to determine the practical applicability of these findings for clinical diagnosis and evaluation.

1. Introduction

Psychiatric studies using neuroimaging techniques (functional magnetic resonance imaging [fMRI] and positron emission tomography [PET]) performed during cognitive activation tasks, such as the verbal fluency task (VFT) (Yurgelun-Todd et al., 1996), n-back task (Driesen et al., 2008; Manoach et al., 1999), and mental arithmetic task (Hugdahl et al., 2004), have consistently shown abnormalities in task-associated activation of the prefrontal cortex (PFC) in patients with schizophrenia (SZ) compared with healthy controls (HCs).

Reduced prefrontal activation during cognitive activation tasks has been observed in patients with major depressive disorder (MDD). However, the abnormal increase or decrease in PFC activation in these patients seems to depend on the type of cognitive task and experimental design. Compared to HCs, patients with MDD were shown to have reduced PFC activation in the VFT (Okada et al., 2003), digit-sorting task (Siegle et al., 2007), AX continuous performance task (Holmes et al., 2005), and emotional task (Liotti and Mayberg, 2001; Mayberg et al., 1999). Conversely, patients with MDD have been reported to have increased activation in the bilateral dorsolateral PFC (DLPFC) during the mental arithmetic task (Hugdahl et al., 2004) and in the left DLPFC during the high-loaded working memory task (Harvey et al., 2005).

Some researchers have compared the functional neuroimaging differences in impaired brain functions between SZ and MDD (Barch et al., 2003; Berman et al., 1993; Holmes et al., 2005; Hugdahl et al., 2004; Walter et al., 2007). Holmes et al. (2005) suggested that patients with SZ and MDD exhibit decreased PFC

* Corresponding author at: Department of Neuropsychiatry, Graduate School of Medicine, The University of Tokyo & MRC Social, Genetic and Developmental Psychiatry Centre, Institute of Psychiatry, King's College London, 7-3-1 Hongo, Bunkyo-ku, Tokyo 113-8655, Japan. Tel.: +81 3 5800 9263; fax: +81 3 5800 6894.
E-mail address: takizawar-tky@umin.ac.jp (R. Takizawa).
[1] These authors contributed equally to this work.

0920-9964/$ – see front matter © 2013 Elsevier B.V. All rights reserved.
http://dx.doi.org/10.1016/j.schres.2013.08.026

activations, although the exact regions involved and extent of signal reduction were different between these patient groups. This led us to expect that apparent similar PFC signal reductions observed for patients with SZ and MDD could be derived from differential neurophysiological findings. These functional brain abnormalities might be valuable for investigating differential brain pathophysiology in different psychiatric disorders. Furthermore, neuroimaging techniques could possibly be promising candidates for translation of imaging-guided differential diagnosis and evaluation into clinical settings.

Recently, the number of neuroimaging studies using near-infrared spectroscopy (NIRS), a relatively new method for investigating cerebral hemodynamic activity, has increased (Ferrari and Quaresima, 2012; Irani et al., 2007). NIRS involves irradiation of near-infrared light into the skull and measuring its reflection from oxy-hemoglobin (oxy-Hb) and deoxy-hemoglobin (deoxy-Hb) (Jobsis, 1977; Koizumi et al., 1999). Compared to other hemodynamic neuroimaging methods (fMRI or PET), NIRS has superior time resolution and inferior spatial resolution and lesser usefulness for detection of deep brain functions. NIRS has the benefits of producing no harmful radiation and being flexible because the NIRS device is compact and portable.

Few fMRI or PET studies have presented the time course of signal change; however, several previous NIRS-based studies have measured time-specific hemodynamic changes in patients with SZ, MDD, and bipolar disorder and clarified the abnormal time course of prefrontal activity in each major psychiatric disorder (Kameyama et al., 2006; Shimodera et al., 2012; Suto et al., 2004). Some of these NIRS studies have also elucidated the association between prefrontal NIRS signals and global functioning levels in psychiatric disorders (Pu et al., 2008; Takizawa et al., 2008). Thus, the specific spatiotemporal characteristics of brain activation patterns in each disorder might become candidate biomarkers of differential brain pathophysiology. However, the previous NIRS studies did not directly compare NIRS signal patterns among different disorders.

In this study, we measured hemodynamic changes during the VFT in patients with SZ and MDD and HCs using concise NIRS measurements in a natural setting. In expansion of a previous study that covered a limited PFC area (Suto et al., 2004), we investigated 3 groups including more subjects ($n = 32$ in each group) with comparable demographic characteristics using a multichannel NIRS machine with a wide coverage over the prefrontal cortical surface area (52 channels, ETG-4000 HITACHI Medical Co.). We also examined the relationship between hemodynamic changes and clinical scores. We hypothesized that the spatiotemporal characteristics of the time course in prefrontal activation patterns differentiate MDD from SZ and are related to global functioning levels in both disorders.

2. Methods

2.1. Participants

This study included 96 individuals: 32 patients with SZ, 32 patients with non-psychotic unipolar MDD, and 32 demographically matched HCs (Table 1). Patients with SZ or MDD did not have any psychiatric comorbidity. The diagnoses of the 2 disorders were established by well-trained psychiatrists (R.T. and K.K.) using DSM-IV criteria. Patients with drug or alcohol dependence and neurological disorders or other organic disorders were excluded. Written informed consent was obtained from all participants. This study was approved by the ethics committees of the University of Tokyo and JR Tokyo General Hospital.

All subjects were right-handed, according to the modified version of the Edinburgh Handedness Inventory (score > 70) (Oldfield, 1971). Participants of each group were matched for age ($F[2, 93] = 1.135$, $p = 0.33$), sex (male:female, 15:17; $p = 1.00$), task performance ($F[2, 93] = 0.113$, $p = 0.33$), and educational level ($F[2, 93] = 1.031$, $p = 0.36$) (Table 1). Hemodynamic response measured by NIRS varies according to the effects of age and sex (Herrmann et al., 2006; Kameyama et al., 2004). Thus, we matched the age and sex of each group to decrease these effects.

Table 1
Clinical characteristics of the study groups.[a]

	Healthy subjects ($n = 32$)	Patients with schizophrenia ($n = 32$)	Patients with depression ($n = 32$)	p value
Sex (male/female)	15/17	15/17	15/17	1.00
Age, years	45.7 ± 13.5	41.7 ± 10.1	44.8 ± 9.8	0.33
Education, years	15.1 ± 2.58	14.9 ± 2.37	14.3 ± 1.91	0.36
Task performance[b]	14.3 ± 3.3	14.8 ± 5.6	13.2 ± 4.7	0.33
PANSS				
Positive	–	15.7 ± 5.00	–	–
Negative	–	22.0 ± 7.11	–	–
General psychopathology	–	38.7 ± 8.47	–	–
HRS-D	–	–	19.6 ± 3.64	–
GAF	–	45.7 ± 14.0	53.3 ± 5.57	–
Medication	–	843 ± 707 (Cp eq. mg)	113 ± 65.7 (Imp eq. mg)	–

Abbreviations: Cp eq., chlorpromazine-equivalent; Imp eq., imipramine-equivalent.
[a] Chi-squared test was used to test group differences in sex distribution. Otherwise, a t test was used.
[b] Number of correct words generated (mean ± SD).

The exclusion criteria for all the groups were neurological illness, traumatic brain injury with any known cognitive consequences or loss of consciousness for more than 5 min, a history of electroconvulsive therapy (Tess and Smetana, 2009), and alcohol/substance abuse or addiction that might be potential confounders for cognitive tasks. An additional exclusion criterion for the control group was a history of psychiatric disease or a family history of axis I disorders in any first-degree relatives. Any patients with MDD and SZ who had other psychiatric or physical comorbidities were excluded. All patients with SZ, a majority of whom had experienced the first or second episode of acute psychotic symptoms and had had the illness for <10 years, were taking various types of antipsychotic medication, including typical and newer atypical antipsychotics. The average dose of antipsychotic medication was 843 ± 707 mg, as a chlorpromazine-equivalent dose. None of the patients with SZ was in an acute phase, but all had some residual psychiatric symptoms at the time of NIRS measurement. Patients with MDD who also met the DSM-IV criteria for a major depressive episode unipolar type were diagnosed by the same well-trained psychiatrists. The total Hamilton Rating Scale for Depression (HRS-D; 17-item version) (Hamilton, 1960) scores of all patients with depression were above 15, which means in a "full symptomatic" state, to confirm the diagnosis and existence of symptoms (Frank et al., 1991). All, except 3, subjects with MDD were taking various types of antidepressants, such as selective serotonin reuptake inhibitors. The average dose of antidepressant medication was 113 ± 65.7 mg, as an imipramine-equivalent dose.

Psychiatric symptoms were rated using the Positive and Negative Syndrome Scale (PANSS) (Kay et al., 1987) in patients with SZ, the HRS-D in patients with MDD, and the Global Assessment of Functioning (GAF) scale in both groups of patients (Table 1).

2.2. Task design

We used the VFT (letter fluency version) as a cognitive task. Previous brain imaging studies have consistently shown abnormal brain activations during the VFT in various psychiatric disorders (Audenaert et al., 2000; Okada et al., 2003; Ragland et al., 2008; Videbech et al., 2003). Participants can be easily instructed on the VFT, and this task has a high successful execution rate for subjects, including psychiatric patients. Recent fMRI studies also used the VFT as a cognitive task; however, the noise in the environment in which the VFT is conducted may influence fMRI measurements. During NIRS measurements, participants are in a silent condition, and hence, observers can expect more natural measurements of cerebral activity induced by VFT using auditory stimuli and utterances.

The whole measurement time was 160 s, including 3 segments (30, 60, and 70 s). Concentration changes for the 2 types of hemoglobin molecules ([deoxy-Hb] and [oxy-Hb]) were measured according to our previous methods (Takizawa et al., 2008, 2009). During the first 30-s and last 70-s segments, participants vocalized 5 Japanese vowels repeatedly, which were used as control tasks. During the middle 60-s interval, the participants were instructed to pronounce in overt speech as many words as possible beginning with the letters indicated by a recorded human voice. To avoid a pause in thinking, the indicated letters were changed every 20 s. Thus, in this 60-s cognitive task period, 3 letters were counterbalanced. The number of words produced throughout the cognitive task period were recorded by an observer and counted as task performance.

2.3. NIRS measurements

The 52-channel NIRS machine (ETG-4000; Hitachi Medical Corporation) measures the relative changes in [oxy-Hb] and [deoxy-Hb] using 2 wavelengths (695 and 830 nm) of infrared light, based on the modified Beer–Lambert law. The distance between pairs of detector probes was set at 3.0 cm. A channel was defined as the measurement area between a pair of source–detector probes. [oxy-Hb] and [deoxy-Hb] changes measured by each of the 52-channel detectors were processed to a numerical value [mM · mm] and recorded on the machine every 0.1 s. Further details of the NIRS have been provided elsewhere (Yamashita et al., 1999).

Subjects placed the plastic frame with the injectors and detectors on their head, covering the bilateral prefrontal area. Using this arrangement, hemodynamic changes could be measured in approximate frontopolar PFC (FPPFC), DLPFC, and ventrolateral PFC (VLPFC) areas (Fig. 1), as corroborated by a multisubject study of anatomical craniocerebral correction using the international 10–20 system.

Furthermore, some studies (Kakimoto et al., 2009; Schecklmann et al., 2008), including ours (Kono et al., 2007), have supported the reliability of multiple NIRS measurements during VFT.

2.4. Statistical analyses

The pre- and post-task baselines were determined as the means across the last 10 s of the pre-task period and the last 5 s of the post-task period, respectively. Linear fitting was performed using the data obtained between the 2 baselines. Moving average methods were applied to remove short-term motion artifacts from the analyzed data (moving average window, 5 s). Since all artifacts were not removed using these methods, we used an algorithm developed previously to automatically reject data with artifacts (see supplementary information in our article Takizawa et al., 2008).

Grand mean waveforms averaged across subjects were created separately for the type of [Hb] and for each group. For parametric statistical tests, the measured [Hb] data from each channel were averaged across the 2 periods (pre-task baseline and 60-s task period).

First, to assess any significant increase in [Hb] associated with the task, we compared the mean [Hb] of the pre-task period and that of the task period at each channel by using Student's paired t tests. As we performed 52 paired t-tests, a correction for multiple comparisons was made using a false-discovery rate (FDR) [two-tailed; we set a value of q that specified the maximum FDR to 0.05, so that there were no more than 5% false-positive results on average (Singh and Dan, 2006)].

For the second analysis, to investigate intergroup differences among the significant channels, we compared the mean [Hb] changes during the task period among the 3 groups for each channel using one-way

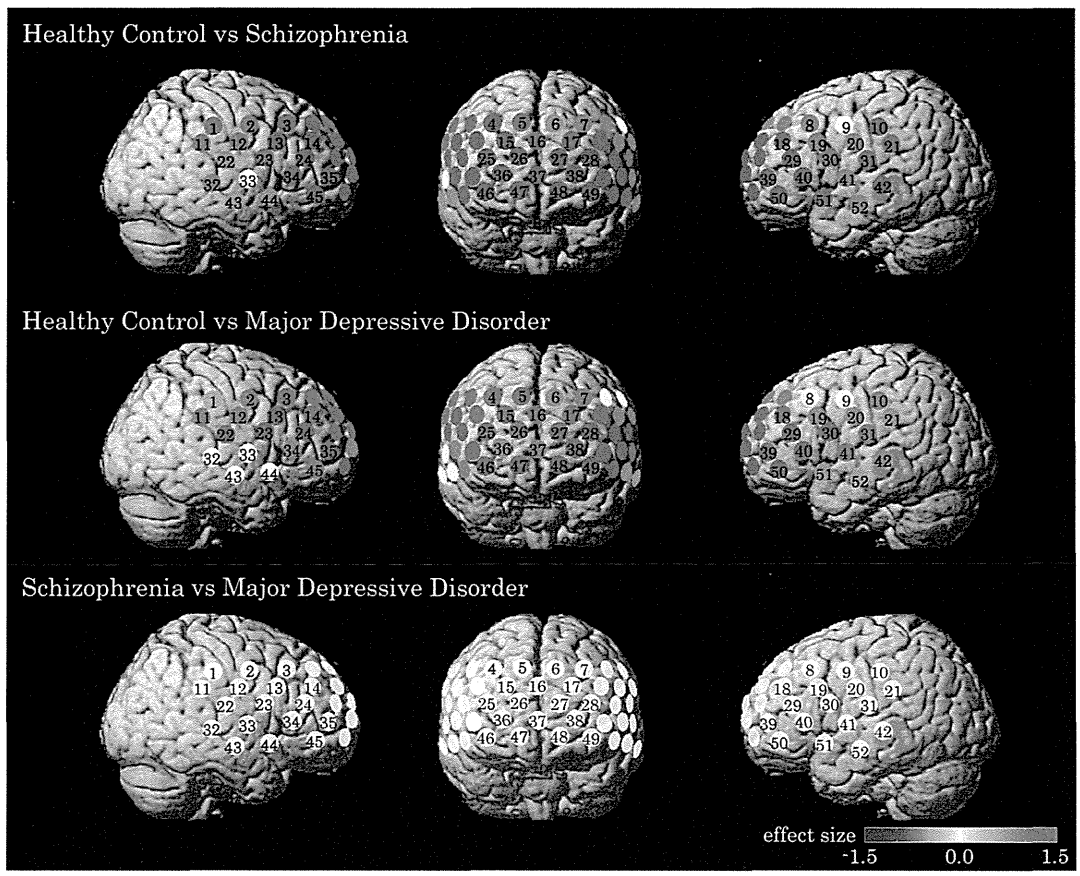

Fig. 1. Group differences in mean [oxy-Hb] increase during the task period. The effect sizes of the group differences are indicated by the color gradient. Channels that did not display significant differences among the 3 groups are colored in white.

analysis of variance (ANOVA); a correction for multiple comparisons was made using FDR.

Subsequently, as post-hoc analyses, we used Tukey's multiple comparison tests to compare the mean [Hb] changes during the task period for channels considered significant after ANOVA between each group (NC–SZ, NC–MDD, and SZ–MDD). A correction for multiple comparisons was made using FDR. To elucidate the spatiotemporal characteristics of NIRS signals, we calculated the effect size (Cohen, 1988) for each difference in these channels.

Next, we compared the time course of [Hb] changes. A previous NIRS study on difference between patients with SZ and MDD (Suto et al., 2004) did not mention statistical significance, but the figure included seemed to show an NIRS signal difference during the first period of the task in the frontopolar cortex area; therefore, we focused our attention on the initial slope of the task period as one of the parameters for the time-course change. To confirm the characteristics of the time course for each group, the initial 5-s slope of the task period was compared among the 3 groups for each channel, in a similar manner. In addition, we conducted similar analyses by using the other parameters for time-course change, which were introduced by Shimodera et al. (2012).

Finally, we analyzed the relationship between [Hb] changes and clinical characteristics, which included GAF, PANSS, and HRS-D scores, age, and dose of medication by calculating Pearson's correlation coefficients. Initially, we investigated the associations between mean NIRS signal change and the clinical characteristics. If any significant association was found, we confirmed the robustness of such associations by using the raw waveform data along the time course of the NIRS signal. According to the conservative method of Kameyama et al. (2006) and Marumo et al. (2009), in order to avoid multiple comparison errors, channels that yielded data with p values of <0.05 for more than 20 s consecutively (200 comparison time points in NIRS signals) during the measurement were considered to have a significant correlation.

Although we focused on [oxy-Hb] here, we have shown the analyses of [deoxy-Hb] data in Supplementary material (1). All data are expressed as means ± S.D. The significance level was set at alpha = 0.05. Statistical analyses were performed using the statistical packager for the Social Sciences ver. 20.0.0J (IBM, Corp., 2011, Chicago IL).

3. Results

3.1. Task performance

The mean number of correct words during the 60-s VFT was not significantly different among the 3 groups ($F[2, 93] = 1.11$, $p = 0.33$, Table 1).

3.2. NIRS [oxy-Hb] change during the VFT period

To assess the presence of significant activations, we compared the mean [oxy-Hb] change between the pre-task and 60-s task periods. HCs showed a significant increase in all channels of the PFC (FPPFC, DLPFC, and VLPFC) (channels 1–52; FDR $p < 0.05$, corrected for 52 channels). Patients with SZ exhibited a significant increase in the DLPFC and VLPFC (channels 24, 34, 35, 39, 41, 44, 45, 47, 49, 51, and 52; FDR $p < 0.05$, corrected for 52 channels), whereas patients with MDD showed a significant increase in the DLPFC, VLPFC, and part of the FPPFC (channels 1, 13, 14, 16–21, 24–29, and 32–52; FDR $p < 0.05$, corrected for 52 channels).

One-way ANOVA using group as a between-subject factor showed a significant main effect of group on the [oxy-Hb] increase during the 60-s task period in the following 50 channels: 1–8, 10–32, and 34–52 (FDR $p < 0.05$, corrected for 52 channels). An additional analysis was performed to compare the 3 groups within the above-mentioned 50 significant channels.

We found that in the widespread PFC, the [oxy-Hb] change in patients with SZ was significantly more reduced than that in HC (channels 1–8, 10–32, 34–52; FDR $p < 0.05$, corrected with 50 channels, Fig. 1).

Similarly, across the PFC, the [oxy-Hb] change was significantly more reduced in patients with MDD than in HCs (channels 1–7, 10–31, 34–42, and 45–52; FDR $p < 0.05$, corrected with 50 channels, Fig. 1).

Patients with SZ and MDD did not show significant difference in the mean [oxy-Hb] for any channel.

3.3. Time course of cognitive activation

The time-course patterns of [oxy-Hb] and [deoxy-Hb] changes in the left FPPFC (channel 38) vary according to diagnostic group (Fig. 2). The HC and MDD groups showed an immediate increase and regular decrease in [oxy-Hb] during the task. In contrast, the SZ group showed slow increase after the start of the task and immediate decrease after the end of the task period. In addition, this group showed a small increase in [oxy-Hb] during the post-task period.

One-way ANOVA using group as a between-subject factor showed a significant difference in the initial slope during the task period at 29 channels (channels 3, 8, 13–18, 20, 24–29, 34–40, and 45–51; FDR $p < 0.05$, corrected for 52 channels). Similar to the analysis of mean [oxy-Hb] change, an additional analysis to compare each group within these 29 significant channels was performed.

The initial slope for HCs was significantly steeper than that for patients with SZ at 26 channels (channels 3, 13–15, 17–18, 20, 24–29, 34–39, and 45–51; FDR $p < 0.05$, corrected for 27 channels, Fig. 3). However, the slope for patients with MDD was not significantly different from that for HCs at any channel (FDR $p > 0.05$, corrected for 27 channels, n.s.).

The slopes for patients with MDD were significantly steeper than those for patients with SZ at 15 channels located approximately in the FPPFC (channels 25–28, 35–40, 45–48 and 51; FDR $p < 0.05$, corrected for 27 channels, Fig. 3).

The comparisons of parameters between the 3 groups for channel 38 are summarized in Fig. 4.

In Supplementary material (2), we also show the results obtained using the indices that Shimodera et al. (2012) used. In brief, one of the

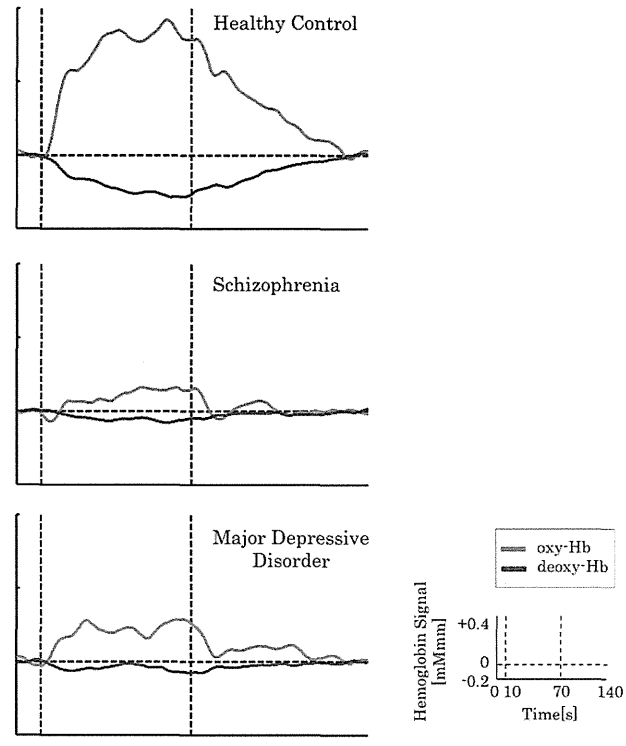

Fig. 2. Time course of [oxy-Hb] and [deoxy-Hb] changes in the FPPFC (channel 38).

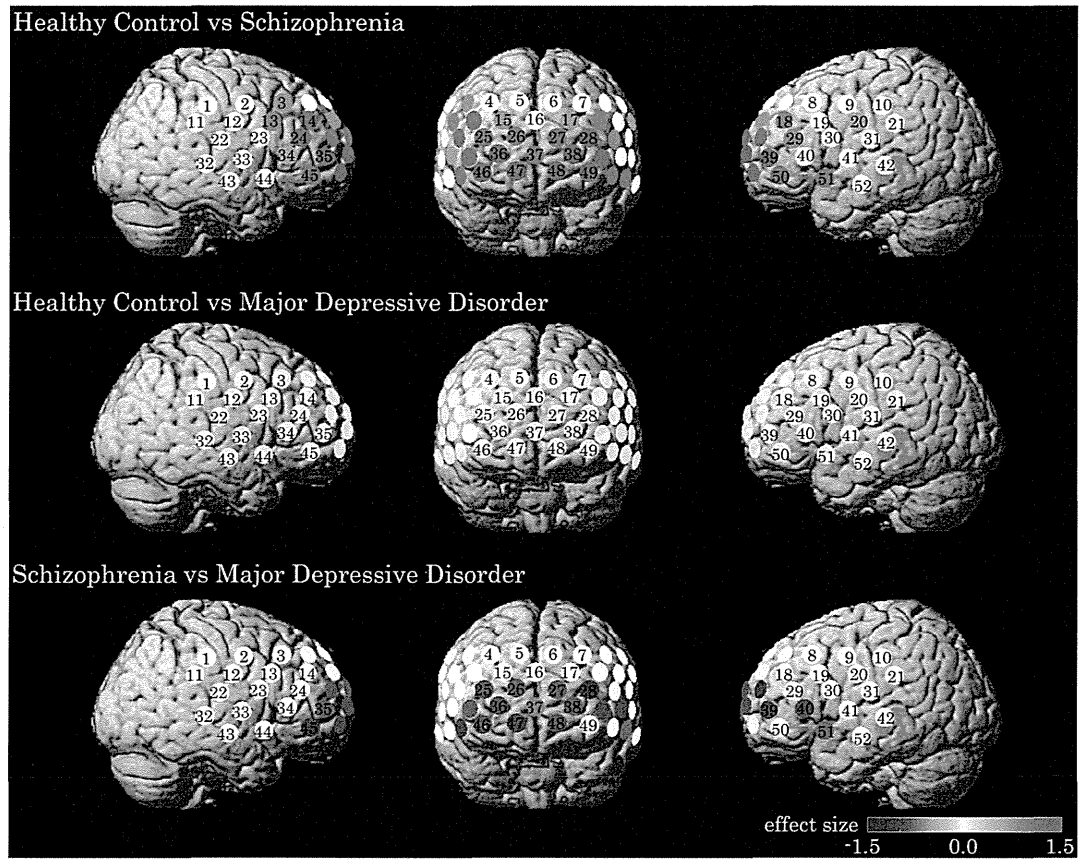

Fig. 3. Group differences in initial [oxy-Hb] slope. The effect sizes of the group differences are indicated by the color gradient. Channels that did not display significant differences among the 3 groups are colored in white.

2 parameters that Shimodera et al. (2012) employed for time-course analysis was significantly different between the patient groups (MDD and SZ) and healthy controls, but not significantly different between the patients with MDD and SZ.

3.4. Correlation with clinical characteristics

For analyzing the correlation between PFC response and clinical characteristics, GAF scores were calculated and found to exhibit significant positive correlations with the mean [oxy-Hb] change of the 60-s task period in patients with SZ at 7 channels ($r = 0.377–0.487$) and in patients with MDD at 23 channels ($r = 0.451–0.610$) (SZ: channels 27–28, 36–39, and 46, located mainly in the FPPFC; MDD: channels 2, 10, 12, 13, 20, 24, 25, 30, 34–37, 39–41, 43, 44, 46–48, and 50–52, located mainly in the DLPFC and VLPFC), which means that the more severe the GAF scores were the more reduced the NIRS changes were (Fig. 5). Additionally, to confirm the robustness of such associations, the time-course analysis of the associations revealed that there were significant associations in the latter half of the time course of the NIRS measurement (SZ: channels 13, 17, 24, 26–28, 34–39, and 46–49, located mainly

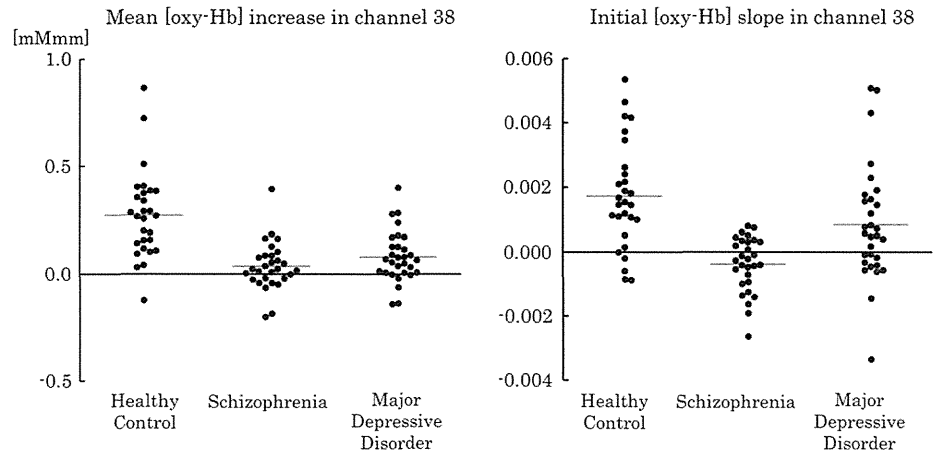

Fig. 4. Comparisons of mean [oxy-Hb] increase and initial [oxy-Hb] slope among the 3 groups. The bars indicate the mean ± 1 standard deviation.

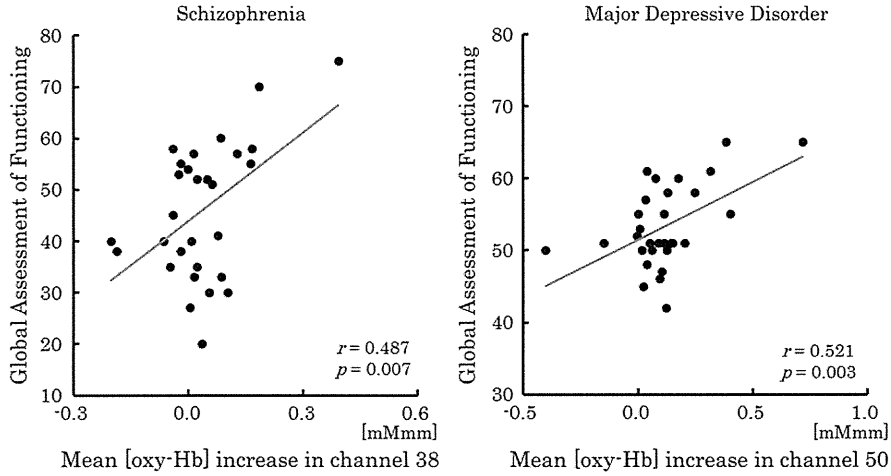

Fig. 5. Scatterplots for correlations between NIRS signal and GAF score in patients with schizophrenia and major depression.

in the FPPFC; MDD: channels 2, 10, 12–13, 20, 24, 29, 34–36, 39–44, 46–48, and 50–52, located mainly in the DLPFC and VLPFC) ($p < 0.05$, with 200 consecutive time points) (Fig. 6).

Other clinical characteristics, including age, dose of medication, and PANSS and HRS-D scores were not significantly correlated with mean [oxy-Hb] change in the 60-s task period at any channel in any group. Moreover, no clinical characteristic showed significant correlation with the initial [oxy-Hb] slope of the task period at any channel in any group.

4. Discussion

These results suggest the presence of a significant difference in the time-course patterns of prefrontal activations in a VFT among HCs, patients with SZ, and patients with MDD matched for age, sex, task performance, and education years. Compared to HCs, patients with SZ and those with MDD showed a significant task-associated reduction in mean [oxy-Hb]. In addition, the initial slope was significantly steeper for patients with MDD and HCs than for patients with SZ. Furthermore, in patients with SZ, the mean [oxy-Hb] change in the area approximately located in the FPPFC was significantly correlated with the GAF score; this is similar to our previous finding (Takizawa et al., 2008), whereas patients with MDD exhibited a significant correlation between mean [oxy-Hb] change and GAF scores in the areas approximately located in the DLPFC and VLPFC. These findings may help understand the differential brain pathophysiology of SZ and MDD better.

4.1. Functional prefrontal abnormality in patients with SZ and MDD

Compared with HCs, patients with SZ and those with MDD showed a reduced NIRS [oxy-Hb] increase in the 60-s task period at the PFC. This result agrees with those of previous NIRS studies (Kameyama et al., 2006; Suto et al., 2004; Takizawa et al., 2008) and other neuroimaging studies.

The 2 patient groups had an [oxy-Hb] reduction compared to that of HCs in FPPFC and DLPFC; however, patients with MDD showed no significant [oxy-Hb] reduction in VLPFC, whereas patients with SZ did, i.e., compared to patients with MDD, those with SZ had reduced NIRS signals in a wider area (Fig. 1). However, patients with SZ and MDD did not show significant difference in mean [oxy-Hb] change at all channels; this suggests that differentiating between these 2 disorders using only the mean change in NIRS signal is difficult.

The VFT recruits not only a single specific cognitive domain, but also some integrated cognitive dimensions, such as working memory,

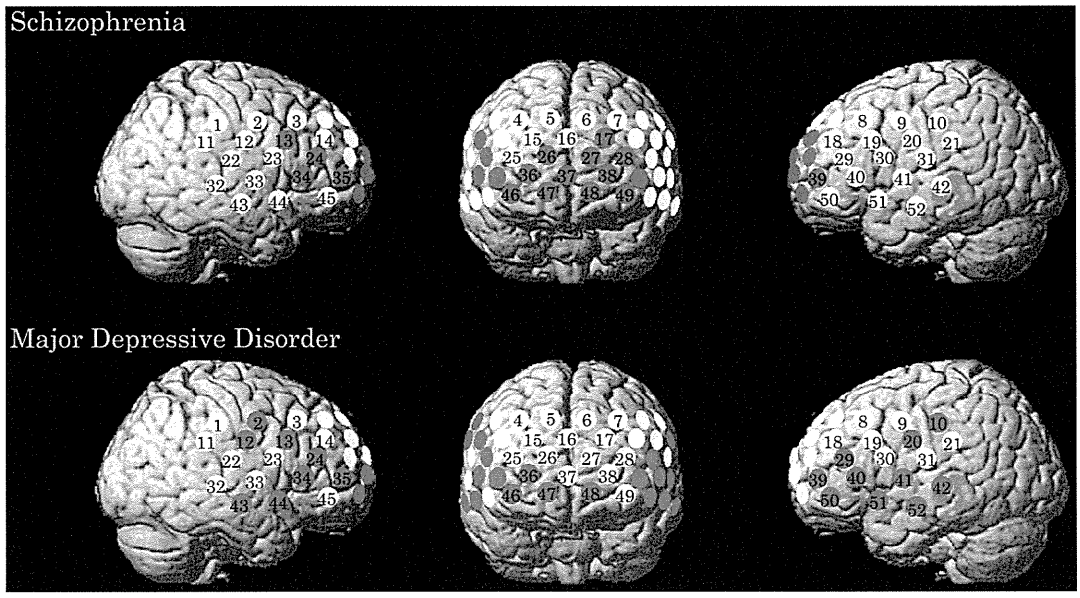

Fig. 6. Cerebral regions that exhibited a significant correlation between GAF score and mean [oxy-Hb] change.

selection of appropriate words, inhibition of inappropriate words, and maintenance of attention (Ruff et al., 1997). For this reason, our "hypofrontality" result during the VFT could not clarify the specific deficit of neural networks in each patient group. However, the difference in mean [oxy-Hb] change during the VFT between patients and HCs may reflect a common impairment, such as executive dysfunction. In addition, from the perspective of the area that showed a group difference (Fig. 1), the brain pathophysiology involving this impairment in SZ might be severer than that of MDD.

4.2. Differential spatiotemporal characteristics of prefrontal activation

The comparison of the time course of [oxy-Hb] signal between the 3 groups (Fig. 2) revealed that the SZ group showed a more gradual slope than the MDD or NC groups, whereas the MDD and HC groups showed no significant difference in the initial slope, immediately after the task started.

Despite the fact that the 2 patient groups had a similar reduced [oxy-Hb] change, there was a difference in the time course of NIRS [oxy-Hb] signal between them. Several previous functional neuroimaging studies based on fMRI also reported a difference in cognitive activation, and the possibilities of qualitative changes, between patients with SZ and MDD (Holmes et al., 2005; Hugdahl et al., 2004). In our study, we replicated this qualitative difference between the disorders based not only on the activation of the PFC region, but also on the comparison of the time course of frontal activation. These findings suggest that the brain pathophysiology of SZ might be severer than that of MDD.

Furthermore, the initial rise rate of the prefrontal hemodynamic response to the task stimulus in patients with MDD was similar to that of HCs, but the response did not continue to increase throughout the task period (Fig. 2), which means that, despite the fact that the load of the task continued, the prefrontal hemodynamic response in these patients did not follow. This discontinuance in the frontal hemodynamic response may reflect symptoms of depression, such as impaired concentration and psychomotor slowing (Hickie et al., 2007). Conversely, patients with SZ appeared to have an inefficient small reactivation or a delay of baseline reversion after the task period (Fig. 2), similar to the results of previous NIRS studies (Suto et al., 2004; Takizawa et al., 2008). As was also discussed for the abnormal time course of patients with SZ observed in a recent NIRS study (Shimodera et al., 2012), only its reduced mean signal change does not seem to represent their functional dysfunctions. The time-course analyses of cognitive activation according to patient groups need to be replicated in future NIRS studies.

4.3. Association between functional impairment and PFC subregions

In this study, we found a significant correlation between the mean [oxy-Hb] change of the task period in specific cerebral regions and the GAF score. However, the correlated cerebral regions were spatially different between patients with SZ (mainly in the FPPFC) and patients with MDD (mainly in the VLPFC/DLPFC) (Fig. 6).

Recent neuroimaging studies reported that the regions activated in patients with SZ were different from those activated in patients with MDD for the same cognitive task, suggesting that the abnormal neural correlates and compensatory mechanisms might be different between patients with SZ and MDD (Barch et al., 2003; Holmes et al., 2005; Hugdahl et al., 2004). Thus, in the present study, the activated regions that correlated to GAF might be variable in each patient group.

Our previous study (Takizawa et al., 2008) was replicated regarding the relationship between GAF score and NIRS [oxy-Hb] increase in the FPPFC and DLPFC. As was discussed in Takizawa et al. (2008), this relationship suggests that reduced frontopolar cortical activations may be associated with functional impairment in patients with SZ.

Regarding patients with MDD, a previous NIRS study using the same VFT (Pu et al., 2008) showed that the mean [oxy-Hb] change in the right DLPFC was significantly associated with scores on the Social Adaptation Self-Evaluation Scale, which evaluates social motivation and behavior (Bosc et al., 1997). This measure should be strongly related with global social functioning, which is similar to what was measured by the GAF scale in the current study. Therefore, here we replicated part of the Pu et al. (2008) regarding the correlations between the DLPFC signal and the generalized scores of social functioning in patients with MDD.

Studies based on nonhuman primates reported that the VLPFC receives projections from the orbitofrontal cortex and subcortical areas, such as the midbrain and amygdala, which are involved in processing motivational and emotional information. The VLPFC might integrate cognitive and motivational information to guide flexible goal-directed behavior (Sakagami and Pan, 2007). In mood disorders, a deficit in the VLPFC observed in emotion tasks reflected the impairment in processing motivational and emotional information in this area (Johnstone et al., 2007; Taylor Tavares et al., 2008). These VLPFC functions may be factors that influence the extent of social functioning in patients with depression. Thus, our results of increasing severity in functional impairments with the reduction of VLPFC signals might be justified. However, the global role of the VLPFC and its relation to social impairment in patients with MDD remains to be elucidated. Our results regarding the VLPFC warrant further investigation.

The correlation between lateral PFC activation and GAF score in patients with MDD suggests that this region plays a key role in maintaining social function in these patients; however, these PFC areas seemed to be different from those observed in patients with SZ, for some reason (e.g., compensatory or abnormal mechanisms). These findings suggest not only differential brain pathophysiology, but also differential symptomatology between patients with MDD and SZ. Further detailed investigations need to be performed in the future.

4.4. Limitations

Some methodological limitations need to be addressed. First, all patients were taking medication at the time of NIRS measurement. Some authors have mentioned an absence of significant effects of psychotropic medications on abnormal structural and functional neuroimaging measures (Phillips et al., 2008). Moreover, similar to what was observed in previous NIRS studies (Shimodera et al., 2012; Takizawa et al., 2008), psychotropic medication dose was not related to [oxy-Hb] change at any channels in the present study. However, the effect of antidepressants or antipsychotics on neuroimaging studies could not be entirely ruled out. In addition, we confirmed that the significant findings were unchanged if either or medication or task performance was included as a covariate in the analyses. Second, in the current study, NIRS measurements were made once throughout the stages of the disease. To repeat the NIRS measurements during the treatment of patients, the actual state of activation patterns throughout the process of recovery may become clear (Walsh et al., 2007). A longitudinal study is needed to replicate our findings. Third, NIRS has a low spatial resolution, and its accuracy in the estimation of measurement positions is limited. According to the virtual registration method (Tsuzuki et al., 2007; Tzourio-Mazoyer et al., 2002), which estimates the cortical localization of each channel. We interpreted that the correlated cerebral area (including channel 24 or 29, and more lateral channels) in patients with MDD was located mainly in the bilateral VLPFC and right DLPFC (Fig. 6).

4.5. Conclusions and future implications

In conclusion, we investigated the hemodynamic changes using the LFT in patients with MDD and SZ and in HCs by using 52-channel NIRS with a wide coverage over the prefrontal cortical surface area. The comparison between patients with SZ and MDD revealed a difference in the time course of the NIRS signal. We also observed a correlation between the GAF score and the mean [oxy-Hb] change at the FPPFC in patients with SZ, and at the DLPFC and VLPFC in patients with MDD. These

results suggest the presence of differential prefrontal abnormalities in each disease, despite a similar reduction in the magnitude of hemodynamic activations between them. These findings may lead to a better understanding of the different brain pathophysiology of SZ and MDD. Finally, these results, if replicated using large-scale or longitudinal studies, suggest that NIRS could potentially be used as an aid for the diagnosis and clinical evaluation of SZ and MDD.

Supplementary data to this article can be found online at http://dx.doi.org/10.1016/j.schres.2013.08.026.

Role of funding source

This work was supported in part by Grants-in-Aid for Scientific Research (Innovative areas No. 23118001 & 23118004 [Adolescent Mind & Self-Regulation] to KK; No. 23791309 to RT) and a grant from the "Development of Biomarker Candidates for Social Behavior" study carried out under the Strategic Research Program for Brain Sciences (to KK) of the MEXT. This study was also supported in part by the Health and Labor Sciences Research Grants for Comprehensive Research on Disability Health and Welfare (H23-seishin-ippan-002 to RT); an Intramural Research Grant for Neurological and Psychiatric Disorders of NCNP (No. 23-10 to RT); and by the Japan Research Foundation for Clinical Pharmacology (to RT). The sponsors had no role in the study design, data collection, data analysis, data interpretation, or writing of the report. The corresponding author had full access to all data in this study, and had the final responsibility in the decision to submit this work for publication.

Contributors

Masato Fukuda, Ryu Takizawa, and Kiyoto Kasai designed the study and wrote the protocol. Ryu Takizawa, Masaru Kinou, and Shingo Kawasaki performed the statistical analysis. Masaru Kinou, Ryu Takizawa, Marumo Kohei, and Yuki Kawakubo carried out data acquisition. Ryu Takizawa and Masaru Kinou wrote the first draft of the manuscript, and the other authors revised it critically for important intellectual content. All authors have approved the final version of the manuscript.

Conflict of interest

Regarding financial and material support for the present study, Dr. Kasai has a potential conflict of interest (see below for details). All other authors have no relevant conflicts of interest.

Beginning July 31, 2003, and continuing to the present, the University of Tokyo and the Hitachi Group (Advanced Research Laboratory, Hitachi Ltd. and The Research and Developmental Center, Hitachi Medical Corporation) have had an official contract for a collaborative study on the clinical applications of near-infrared spectroscopy (NIRS) in psychiatric disorders, which has been approved by the Research Promotion Office, University of Tokyo Hospital. The principal investigator of this study is Kiyoto Kasai. For this study, the Hitachi Medical Corporation provided a project grant (JPY 300,000 per year) and material support (temporary rental of a near-infrared spectroscopy machine (ETG-4000, Optical Topography)).

Acknowledgments

The authors thank all the participants in this study. This study is based in part on the Ph.D. thesis of Dr. Kinou, which was submitted to the University of Tokyo.

References

Audenaert, K., Brans, B., Van Laere, K., Lahorte, P., Versijpt, J., van Heeringen, K., Dierckx, R., 2000. Verbal fluency as a prefrontal activation probe: a validation study using 99mTc-ECD brain SPET. Eur. J. Nucl. Med. 27 (12), 1800–1808.

Barch, D.M., Sheline, Y.I., Csernansky, J.G., Snyder, A.Z., 2003. Working memory and prefrontal cortex dysfunction: specificity to schizophrenia compared with major depression. Biol. Psychiatry 53 (5), 376–384.

Berman, K.F., Doran, A.R., Pickar, D., Weinberger, D.R., 1993. Is the mechanism of prefrontal hypofunction in depression the same as in schizophrenia? Regional cerebral blood flow during cognitive activation. Br. J. Psychiatry 162, 183–192.

Bosc, M., Dubini, A., Polin, V., 1997. Development and validation of a social functioning scale, the social adaptation self-evaluation scale. Eur. Neuropsychopharmacol. 7 (Suppl. 1), S57–70 (discussion S71-53).

Cohen, J., 1988. Statistical Power Analysis for the Behavioral Sciences, 2nd ed. Erlbaum, Hillsdale, NJ.

Driesen, N.R., Leung, H.C., Calhoun, V.D., Constable, R.T., Gueorguieva, R., Hoffman, R., Skudlarski, P., Goldman-Rakic, P.S., Krystal, J.H., 2008. Impairment of working memory maintenance and response in schizophrenia: functional magnetic resonance imaging evidence. Biol. Psychiatry 64 (12), 1026–1034.

Ferrari, M., Quaresima, V., 2012. A brief review on the history of human functional near-infrared spectroscopy (fNIRS) development and fields of application. Neuroimage 63 (2), 921–935.

Frank, E., Prien, R.F., Jarrett, R.B., Keller, M.B., Kupfer, D.J., Lavori, P.W., Rush, A.J., Weissman, M.M., 1991. Conceptualization and rationale for consensus definitions of terms in major depressive disorder. Remission, recovery, relapse, and recurrence. Arch. Gen. Psychiatry 48 (9), 851–855.

Hamilton, M., 1960. A rating scale for depression. J. Neurol. Neurosurg. Psychiatry 23, 56–62.

Harvey, P.O., Fossati, P., Pochon, J.B., Levy, R., Lebastard, G., Lehericy, S., Allilaire, J.F., Dubois, B., 2005. Cognitive control and brain resources in major depression: an fMRI study using the n-back task. NeuroImage 26 (3), 860–869.

Herrmann, M.J., Walter, A., Ehlis, A.C., Fallgatter, A.J., 2006. Cerebral oxygenation changes in the prefrontal cortex: effects of age and gender. Neurobiol. Aging 27 (6), 888–894.

Hickie, I.B., Naismith, S.L., Ward, P.B., Little, C.L., Pearson, M., Scott, E.M., Mitchell, P., Wilhelm, K., Parker, G., 2007. Psychomotor slowing in older patients with major depression: relationships with blood flow in the caudate nucleus and white matter lesions. Psychiatry Res. 155 (3), 211–220.

Holmes, A.J., MacDonald III, A., Carter, C.S., Barch, D.M., Andrew Stenger, V., Cohen, J.D., 2005. Prefrontal functioning during context processing in schizophrenia and major depression: an event-related fMRI study. Schizophr. Res. 76 (2–3), 199–206.

Hugdahl, K., Rund, B.R., Lund, A., Asbjornsen, A., Egeland, J., Ersland, L., Landro, N.I., Roness, A., Stordal, K.I., Sundet, K., Thomsen, T., 2004. Brain activation measured with fMRI during a mental arithmetic task in schizophrenia and major depression. Am. J. Psychiatry 161 (2), 286–293.

Irani, F., Platek, S.M., Bunce, S., Ruocco, A.C., Chute, D., 2007. Functional near infrared spectroscopy (fNIRS): an emerging neuroimaging technology with important applications for the study of brain disorders. Clin. Neuropsychol. 21 (1), 9–37.

Jobsis, F.F., 1977. Noninvasive, infrared monitoring of cerebral and myocardial oxygen sufficiency and circulatory parameters. Science 198 (4323), 1264–1267.

Johnstone, T., van Reekum, C.M., Urry, H.L., Kalin, N.H., Davidson, R.J., 2007. Failure to regulate: counterproductive recruitment of top-down prefrontal-subcortical circuitry in major depression. J. Neurosci. 27 (33), 8877–8884.

Kakimoto, Y., Nishimura, Y., Hara, N., Okada, M., Tanii, H., Okazaki, Y., 2009. Intrasubject reproducibility of prefrontal cortex activities during a verbal fluency task over two repeated sessions using multi-channel near-infrared spectroscopy. Psychiatry Clin. Neurosci. 63 (4), 491–499.

Kameyama, M., Fukuda, M., Uehara, T., Mikuni, M., 2004. Sex and age dependencies of cerebral blood volume changes during cognitive activation: a multichannel near-infrared spectroscopy study. NeuroImage 22 (4), 1715–1721.

Kameyama, M., Fukuda, M., Yamagishi, Y., Sato, T., Uehara, T., Ito, M., Suto, T., Mikuni, M., 2006. Frontal lobe function in bipolar disorder: a multichannel near-infrared spectroscopy study. NeuroImage 29 (1), 172–184.

Kay, S.R., Fiszbein, A., Opler, L.A., 1987. The positive and negative syndrome scale (PANSS) for schizophrenia. Schizophr. Bull. 13 (2), 261–276.

Koizumi, H., Yamashita, Y., Maki, A., Yamamoto, T., Ito, Y., Itagaki, H., Kennan, R., 1999. Higher-order brain function analysis by trans-cranial dynamic near-infrared spectroscopy imaging. J. Biomed. Opt. 4 (4), 403–413.

Kono, T., Matsuo, K., Tsunashima, K., Kasai, K., Takizawa, R., Rogers, M.A., Yamasue, H., Yano, T., Taketani, Y., Kato, N., 2007. Multiple-time replicability of near-infrared spectroscopy recording during prefrontal activation task in healthy men. Neurosci. Res. 57 (4), 504–512.

Liotti, M., Mayberg, H.S., 2001. The role of functional neuroimaging in the neuropsychology of depression. J. Clin. Exp. Neuropsychol. 23 (1), 121–136.

Manoach, D.S., Press, D.Z., Thangaraj, V., Searl, M.M., Goff, D.C., Halpern, E., Saper, C.B., Warach, S., 1999. Schizophrenic subjects activate dorsolateral prefrontal cortex during a working memory task, as measured by fMRI. Biol. Psychiatry 45 (9), 1128–1137.

Marumo, K., Takizawa, R., Kawakubo, Y., Onitsuka, T., Kasai, K., 2009. Gender difference in right lateral prefrontal hemodynamic response while viewing fearful faces: a multichannel near-infrared spectroscopy study. Neurosci. Res. 63 (2), 89–94.

Mayberg, H.S., Liotti, M., Brannan, S.K., McGinnis, S., Mahurin, R.K., Jerabek, P.A., Silva, J.A., Tekell, J.L., Martin, C.C., Lancaster, J.L., Fox, P.T., 1999. Reciprocal limbic-cortical function and negative mood: converging PET findings in depression and normal sadness. Am. J. Psychiatry 156 (5), 675–682.

Okada, G., Okamoto, Y., Morinobu, S., Yamawaki, S., Yokota, N., 2003. Attenuated left prefrontal activation during a verbal fluency task in patients with depression. Neuropsychobiology 47 (1), 21–26.

Oldfield, R.C., 1971. The assessment and analysis of handedness: the Edinburgh inventory. Neuropsychologia 9 (1), 97–113.

Phillips, M.L., Travis, M.J., Fagiolini, A., Kupfer, D.J., 2008. Medication effects in neuroimaging studies of bipolar disorder. Am. J. Psychiatry 165 (3), 313–320.

Pu, S., Matsumura, H., Yamada, T., Ikezawa, S., Mitani, H., Adachi, A., Nakagome, K., 2008. Reduced frontopolar activation during verbal fluency task associated with poor social functioning in late-onset major depression: multi-channel near-infrared spectroscopy study. Psychiatry Clin. Neurosci. 62 (6), 728–737.

Ragland, J.D., Moelter, S.T., Bhati, M.T., Valdez, J.N., Kohler, C.G., Siegel, S.J., Gur, R.C., Gur, R.E., 2008. Effect of retrieval effort and switching demand on fMRI activation during semantic word generation in schizophrenia. Schizophr. Res. 99 (1–3), 312–323.

Ruff, R.M., Light, R.H., Parker, S.B., Levin, H.S., 1997. The psychological construct of word fluency. Brain lang. 57 (3), 394–405.

Sakagami, M., Pan, X., 2007. Functional role of the ventrolateral prefrontal cortex in decision making. Curr. Opin. Neurobiol. 17 (2), 228–233.

Schecklmann, M., Ehlis, A.C., Plichta, M.M., Fallgatter, A.J., 2008. Functional near-infrared spectroscopy: a long-term reliable tool for measuring brain activity during verbal fluency. NeuroImage 43 (1), 147–155.

Shimodera, S., Imai, Y., Kamimura, N., Morokuma, I., Fujita, H., Inoue, S., Furukawa, T.A., 2012. Mapping hypofrontality during letter fluency task in schizophrenia: a multi-channel near-infrared spectroscopy study. Schizophr. Res. 136 (1–3), 63–69.

Siegle, G.J., Thompson, W., Carter, C.S., Steinhauer, S.R., Thase, M.E., 2007. Increased amygdala and decreased dorsolateral prefrontal BOLD responses in unipolar depression: related and independent features. Biol. Psychiatry 61 (2), 198–209.

Singh, A.K., Dan, I., 2006. Exploring the false discovery rate in multichannel NIRS. NeuroImage 33 (2), 542–549.

Suto, T., Fukuda, M., Ito, M., Uehara, T., Mikuni, M., 2004. Multichannel near-infrared spectroscopy in depression and schizophrenia: cognitive brain activation study. Biol. Psychiatry 55 (5), 501–511.
Takizawa, R., Kasai, K., Kawakubo, Y., Marumo, K., Kawasaki, S., Yamasue, H., Fukuda, M., 2008. Reduced frontopolar activation during verbal fluency task in schizophrenia: a multi-channel near-infrared spectroscopy study. Schizophr. Res. 99 (1–3), 250–262.
Takizawa, R., Hashimoto, K., Tochigi, M., Kawakubo, Y., Marumo, K., Sasaki, T., Fukuda, M., Kasai, K., 2009. Association between sigma-1 receptor gene polymorphism and prefrontal hemodynamic response induced by cognitive activation in schizophrenia. Prog. Neuropsychopharmacol. Biol. Psychiatry 33 (3), 491–498.
Taylor Tavares, J.V., Clark, L., Furey, M.L., Williams, G.B., Sahakian, B.J., Drevets, W.C., 2008. Neural basis of abnormal response to negative feedback in unmedicated mood disorders. NeuroImage 42 (3), 1118–1126.
Tess, A.V., Smetana, G.W., 2009. Medical evaluation of patients undergoing electroconvulsive therapy. N. Engl. J. Med. 360 (14), 1437–1444.
Tsuzuki, D., Jurcak, V., Singh, A.K., Okamoto, M., Watanabe, E., Dan, I., 2007. Virtual spatial registration of stand-alone fNIRS data to MNI space. NeuroImage 34 (4), 1506–1518.
Tzourio-Mazoyer, N., Landeau, B., Papathanassiou, D., Crivello, F., Etard, O., Delcroix, N., Mazoyer, B., Joliot, M., 2002. Automated anatomical labeling of activations in SPM using a macroscopic anatomical parcellation of the MNI MRI single-subject brain. NeuroImage 15 (1), 273–289.
Videbech, P., Ravnkilde, B., Kristensen, S., Egander, A., Clemmensen, K., Rasmussen, N.A., Gjedde, A., Rosenberg, R., 2003. The Danish PET/depression project: poor verbal fluency performance despite normal prefrontal activation in patients with major depression. Psychiatry Res. 123 (1), 49–63.
Walsh, N.D., Williams, S.C.R., Brammer, M.J., Bullmore, E.T., Kim, J., Suckling, J., Mitterschiffthaler, M.T., Cleare, A.J., Pich, E.M., Mehta, M.A., Fu, C.H.Y., 2007. A longitudinal functional magnetic resonance imaging study of verbal working memory in depression after antidepressant therapy. Biol. Psychiatry 62 (11), 1236.
Walter, H., Vasic, N., Hose, A., Spitzer, M., Wolf, R.C., 2007. Working memory dysfunction in schizophrenia compared to healthy controls and patients with depression: evidence from event-related fMRI. NeuroImage 35 (4), 1551–1561.
Yamashita, Y., Maki, A., Koizumi, H., 1999. Measurement system for noninvasive dynamic optical topography. J. Biomed. Opt. 4 (4), 414–417.
Yurgelun-Todd, D.A., Waternaux, C.M., Cohen, B.M., Gruber, S.A., English, C.D., Renshaw, P.F., 1996. Functional magnetic resonance imaging of schizophrenic patients and comparison subjects during word production. Am. J. Psychiatry 153 (2), 200–205.

Schizophrenia Research 143 (2013) 116–124

Contents lists available at SciVerse ScienceDirect

Schizophrenia Research

journal homepage: www.elsevier.com/locate/schres

A multimodal approach to investigate biomarkers for psychosis in a clinical setting: The integrative neuroimaging studies in schizophrenia targeting for early intervention and prevention (IN-STEP) project

Shinsuke Koike [a,b,*], Yosuke Takano [a], Norichika Iwashiro [a], Yoshihiro Satomura [a], Motomu Suga [a], Tatsuya Nagai [a], Tatsunobu Natsubori [a], Mariko Tada [a], Yukika Nishimura [a], Syudo Yamasaki [c,d], Ryu Takizawa [a], Noriaki Yahata [a], Tsuyoshi Araki [d], Hidenori Yamasue [a], Kiyoto Kasai [a,e]

[a] Department of Neuropsychiatry, Graduate School of Medicine, the University of Tokyo, Bunkyo-ku, Tokyo 113-8655, Japan
[b] Office for Mental Health Support, Division for Counseling and Support, the University of Tokyo, Bunkyo-ku, Tokyo 113-0033, Japan
[c] Department of Psychiatry and Behavioral Science, Tokyo Metropolitan Institute of Medical Science, Setagaya-ku 156-8506, Japan
[d] Department of Youth Mental Health, Graduate School of Medicine, the University of Tokyo, Bunkyo-ku, Tokyo 113-8655, Japan
[e] JST, National Bioscience Database Center (NBDC), 5-3, Yonbancho, Chiyoda-ku, Tokyo 102-0081, Japan

ARTICLE INFO

Article history:
Received 9 August 2012
Received in revised form 29 October 2012
Accepted 12 November 2012
Available online 4 December 2012

Keywords:
Schizophrenia
Neuroimaging
Biological markers
Early intervention
Clinical outcome

ABSTRACT

Longitudinal clinical investigations and biological measurements have determined not only progressive brain volumetric and functional changes especially around the onset of psychosis but also the abnormality of developmental pathways based on gene–environment interaction model. However, these studies have contributed little to clinical decisions on their diagnosis and therapeutic choices because of subtle differences between patients and healthy controls. A multi-modal approach may resolve this limitation and is favorable to explore the pathophysiology of psychosis. The integrative neuroimaging studies for schizophrenia targeting early intervention and prevention (IN-STEP) is a research project aimed at exploring the pathophysiological features of the onset of psychosis and investigating possible predictive biomarkers for the clinical treatment of psychosis. Since 2008, we have adopted blood sampling, neurocognitive batteries, neurophysiological assessment, structural imaging, and functional imaging longitudinally for help-seeking ultra-high-risk (UHR) individuals and patients with first-episode psychosis (FEP). Here, we intend to introduce the IN-STEP research study protocol and present preliminary clinical findings. Thirty-seven UHR individuals and 30 patients with FEP participated in this study. Six months later, there was no difference in objective and subjective scores between the groups, which suggests that young people having symptoms and functional deficits should be cared for regardless of their history of psychosis according to their clinical stages. The rate of transition to psychosis was 7.1%, 8.0%, and 35.3% (at 6, 12, and 24 months, respectively). Through this research project, we expect to clarify the pathophysiological features around the onset of psychosis and improve the prognosis of psychosis through clinical application.

1. Introduction

Longitudinal clinical investigations and neuropsychological, neurophysiological, and neuroimaging measurements have helped to elucidate the pathophysiological features of schizophrenia (Insel, 2010). Recent studies have shown the abnormality of developmental pathways based on gene–environment interaction model and progressive brain volumetric and functional changes especially around the onset (Insel, 2010; van Os et al., 2010). However, these studies have contributed little to clinical decisions on their diagnosis and therapeutic choices until now (Borgwardt and Fusar-Poli, 2012). One possible problem is that most of the methods and instruments applied have substantial limitations and cannot clearly illustrate detailed and schematic brain changes, because differences between patients and healthy controls are subtle. Replication studies and more sophisticated methods are required to provide good reliability and validity prior to clinical application.

Multi-modal approaches may resolve these limitations and reveal the specific pathophysiology of psychosis (Salisbury et al., 2007; Prata et al., 2009; Takizawa et al., 2009; Fusar-Poli et al., 2010, 2011b). For example, several imaging genetic studies have suggested that variations in the catechol-*O*-methyltransferase genotype have different effects on the frontal cortical function in patients with schizophrenia and healthy controls (Prata et al., 2009; Takizawa et al., 2009). A previous longitudinal multi-modal imaging study indicated that

* Corresponding author at: Office for Mental Health Support, Division for Counseling and Support, the University of Tokyo, Yasuda-Auditorium, 7-3-1 Hongo, Bunkyo-ku, Tokyo 113-0033, Japan. Tel.: +81 3 5841 2578; fax: +81 3 5800 6894.
E-mail address: skoike-tky@umin.ac.jp (S. Koike).

0920-9964/$ – see front matter © 2012 Elsevier B.V. All rights reserved.
http://dx.doi.org/10.1016/j.schres.2012.11.012